6-2017

Red Grain Sorghum Whole Kernel Crude Lipid Protects Energy Metabolism And Short Chain Fatty Acid Profile In A Hamster Model To Minimize Intestinal Stress Caused By A High Fat Diet

Haowen Qiu
University of Nebraska-Lincoln, ytqiuhaowen@gmail.com

Red grain sorghum whole kernel crude lipid protects energy metabolism and short chain fatty acid profile in a hamster model to minimize intestinal stress caused by a high fat diet

By

Haowen Qiu

A THESIS

Presented to the Faculty of

The Graduate College at the University of Nebraska

In Partial fulfillment of Requirements

For the Degree of Master of Science

Major: Nutrition

Under the Supervision of Professor Vicki Schlegel

Lincoln, Nebraska

June, 2017

Red grain sorghum whole kernel crude lipid protects energy metabolism and short chain fatty acid profile in a hamster model to minimize intestinal stress caused by a high fat diet

Haowen Qiu, M.S.

University of Nebraska, 2017

Advisor: Vicki Schlegel

Multiple studies have shown throughout the past 10+ years that grain sorghum (GS) lipid extract protects against high plasma and hepatic cholesterol and, to a lesser degree, positively modulate the gut microbiota in response to a high fat (HF) diet. However, the impact of GS lipids on intestinal stress induced by such a diet remains largely unknown. The objective of this project was to determine the ability of GS crude lipid (GS-CL) obtained from the surface of GS whole kernel to protect energy metabolism and short chain fatty acid (SCFA) profile produced by the gut microbiome that may be negatively affected by a HF diet. If left unchecked, such impacts can lead to hypoxia or inflammation and thereby other chronic conditions. In our study, male hamsters were fed with either a low fat control diet, a HF diet or a HF diet supplemented with 1, 3, 5% (w/w) GS-CL for four weeks. The hamsters were then euthanized and the large intestine obtained and analyzed using targeted metabolomics. Analysis of central carbon metabolites showed that the HF diet impaired energy generation and disrupted cellular redox balance. A significant increase of many intermediates of glycolysis (particularly glyceraldehyde-3-phosphate, glycerate-3-phosphate and phosphoenolpyruvate) and tricarboxylic acid (TCA) cycle (particularly succinate, fumarate and malate) occurred in response to a HF influence, while nearly all amino acids were significantly lower compared to the low fat diet. The GS-CL supplements were able to maintain energy levels in the large intestine, especially the 1 and 3% but were not able to rebalance redox equilibrium completely. Moreover, multivariant analysis including orthogonal-partial least squares-discrimination analysis (OPLS-DA) demonstrated that the GS-CL

supplements were able to gradually maintain the HF affected metabolites to levels trending or comparable to the control level, with 3% supplement being the optimal diet in this regard. In general, the data indicated that the GS-CL supplements slowed down the gluconeogenesis and anaplerosis from pyruvate and amino acids, which in turn mitigated the accumulation of glycolysis and TCA intermediates in a dose-depended manner. In addition, the GS-CL supplements positively affected the short chain fatty acid (SCFA) produced by large intestine microbiome, with the 3% diet again exerting the optimal protection, against HF induced changes in SCFA profile followed by 1% supplement. Synergistic interaction among various components in GS-CL (such as the characterized phytosterols and policosanols) may be responsible for some of the metabolic responses as the effects of GS-CL is optimal compared to that reported of the GS oil or wax fraction alone. This study is the first to provide whole-scale impact of GS-CL on cellular energy and central carbon metabolism using a combined approach of metabolomics and multivariant analysis, which effectively demonstrate the potentials of GS-CL as a supplement to prevent or contain chronic metabolic diseases.

Acknowledgement

First and foremost, I want to express my sincerest gratitude to my advisor Dr. Vicki Schlegel. She is not only my teacher and supervisor, guild me through my Master study, but also a close friend and my mentor. She aspired me with her critical thinking, her outstanding professional knowledge and skills, and also as an independent modern feminist. I also want to thank my committee member Dr. Timothy Carr and Dr. Curtis Weller for the guidance and advices they gave me when I faced problems with my experiments. I remember the afternoon in Dr. Carr's office as he explained to us how to do an animal study step by step. I also want to thank Dr. Weller for his contribution in the field of grain sorghum research, most of my knowledge about grain sorghum comes from his papers. I also want to thank Dr. Javier Seravalli for his help with sugar phosphate analysis. When I visited him in his lab, he took the afternoon teaching me every instrument he had. I am tremendously fortunate to have the opportunity to work with and learn from you all.

I also want to thank my fellow lab partners and close friends Sami Althwab and An Nguyen for their help on animal care and sample collection. It was my great honor to work alongside you two and I benefited greatly from our talks and discussions. Since I joined our lab, my lab mates assisted me graciously with daily lab procedures and helped me blend in sooner than I expected. I also want to give special thanks to our lab manager Richard Zbasnik, not only for your help with the characterization of sorghum lipids, but also for your continuous support and care he showed for all our lab mates.

At last, I want to thank my parents. They raised me to become the person I am and provide me a chance to pursue my academic career in the U.S. and to meet all the excellent people above. They reminded me with every phone call and every message just how loved and blessed I am. I love you.

Contents

List of Figures

List of Tables

1. Literature review

I. Introduction to grain sorghum (GS)

Sorghum *(Sorghum bicolor (L.) Moench)*, in the form of a grain, forage or sugar crop, is the fifth most important cereal in the world succeeded only by wheat, rice, maize and barley (Althwab, Carr, Weller, Dweikat, & Schlegel, 2015). Currently, sorghum is widely cultivated in more than 30 countries due to its tolerance to temperature and moist fluctuations, thereby providing food for over 500 million people (Rooney, et al., 2010). For the United States, grain sorghum (GS) acreage has ranged from 15 to 18 million acres per year during the past 25 years (Carter, et al., 2016), which is slightly greater than land dedicated to oat and barley production. In 2011, the U.S was the No. 1 exporter and the No. 2 producer (behind Nigeria) of GS with Kansas, Arkansas, Nebraska, Colorado and Missouri being the primary GS growers among the 21 states that produce sorghum according to the U.S. Department of Agriculture (2016).

Yet, GS has been mainly used as animal feeds in the U.S., but more recently interest has been growing in employing GS as a source for biofuel production (Wang, Weller, & Hwang, 2005). This lack of GS consumption in the U.S. is regrettable as GS contains a unique phytochemical profile, including phenolic acids, condensed tannins, anthocyanins, policosanols and phytosterols (Awika & Rooney, 2004). Indeed, numerous studies on these compounds using both an in vitro and in vivo approaches have shown their antioxidant and anti-inflammatory effects as well as their health benefiting properties on weight control, glycemic control and gut microbiota as will be discussed in the next sections of this chapter.

A. Composition and potential health benefits of grain sorghum

Grain sorghum provides a rich source of health promoting agents (nutraceuticals) for the human diet. The main components present in GS include starch (~75%), protein (~12%), lipids (~4%), fiber (~7%) and several minerals and vitamins (Althwab, Carr, Weller, Dweikat, & Schlegel, 2015) (Stefoska-Needham, Beck, Johnson, & Tapsell, 2015). Additionally, GS

possesses a unique phytochemical profile, including ample types of phytosterols, policosanols and phenolic compounds, which are often considered the components responsible for the many health benefits associated with GS (Awika & Rooney, 2004) (de Morais Cardoso, Pinheiro, Martino, & Pinheiro-Sant'Ana, 2017).

i. Antioxidant

Grain sorghum exhibits significantly antioxidant activity as reported throughout the literature. For example, feeding high tannin sorghum to rats reduced markers of protein oxidation in the muscle without affecting animal growth (Larrain, Richards, Schaefer, & Reed, 2007). During colon carcinogenesis, rats fed a black sorghum bran diet presented with increased activity of colon-based superoxide dismutase (SOD), while rats fed white sorghum bran exhibited elevated catalase (CAT) activity. These results indicate that the sorghum diet is able to increase key endogenous antioxidant enzymes to protect against oxidative stress (Lewis, et al., 2008). Oboh et al. (2010) also confirmed the antioxidant properties of sorghum by demonstrating the neuroprotective effect of a red dye fraction obtained from a sorghum extract against cyclophosphamide-induced oxidative stress using a rat clinical model. The protective effect was attributed to the antioxidant activities exerted by the high phenolic components present in the red dye. In addition, cisplatin-induced nephrotoxicity and hepatotoxicity were remediated by a sorghum straw and a leaf sheath dye supplement, respectively, which occurred by reversing elevated plasma, kidney and liver antioxidant indices (Ademiluyi, Oboh, Agbebi, & Oyeleye, 2014). Moreover, Ajiboye et al. (2013) demonstrated that a sorghum phenolic rich extract protected rat microsomes against diethylnitrosamine (DEN)-induced redox imbalance by significantly attenuating a DEN-mediated decrease in the activities of redox oxygen species (ROS) detoxifying enzymes. Recently, a human clinical trial using healthy subjects studied the antioxidative effect of consuming pasta containing sorghum flour. The sorghum treated group presented with significantly higher plasma polyphenols, antioxidant capacity, SOD activity and lower protein carbonyl levels compared to control group, indicating an enhanced antioxidant

status and improved markers of oxidative stress (Khan, Yousif, Johnson, & Gamlath, 2015). Lastly, Cruz et al. (2015) showed that a sorghum kafirin extract resulted in higher proportion of α-kafirin monomers and hydrophobic amino acid content, which in turn has been linked to improved lipid metabolism and increased serum antioxidant potential in rats.

ii. Anti-inflammation

Reports have further shown that GS exerts anti-inflammatory effects, which again has been attributed to the presence of a variety of phytochemicals, especially those present in the bran. One such study compared the impact of hyaluronidase, which has been correlated with chronic inflammation, in response to extracts obtained from wheat and rice bran and from brans originating from six varieties of sorghum (Bralley, Greenspan, Hargrove, & Hartle, 2008). The sorghum extracts were more effective in inhibiting hyaluronidase activity in vitro compared to its counterparts. The responses were positively correlated to total phenolic content and ferric reducing antioxidant power values. The researchers proposed that this inhibitory effect supports the development of sorghum bran as an anti-inflammatory nutraceutical (Bralley, Greenspan, Hargrove, & Hartle, 2008). Burdette et al. (2007; 2010) also tested the anti-inflammatory effect of sorghum bran extracts in a 12-O-tetradecanoylphorbol acetate (TPA)-induced ear edema rat model. The extract of black sorghum bran significantly decreased ear thickness and weights of ear punches after TPA treatment in addition to inhibiting the secretion of the pro-inflammatory cytokines interleukin 1-beta (IL-1β) and tumor necrosis factor alpha (TNF-α) (Burdette, Hargrove, Hartle, & Greenspan, 2007) (Burdette, et al., 2010). Another study using the extract of golden gelatinous sorghum bran showed that the expression level of cyclooxygenase 2 (COX-2) and inducible nitric oxide synthase (iNOS) induced by 12-O-tetradecanoylphorbol-13-acetate (TPA) were inhibited in a rat model (Shim, Kim, Jang, Ko, & Kim, 2013). Additionally, Hartle, Greenspan, and Hargrove (2011) showed that the anti-inflammatory activity of the black sorghum brans correlated with their phenolic content and antioxidant activity. Ritchie et al. (2011) also reported that a black sorghum bran containing diet was able to remediate dextran sulfate sodium

(DSS)-induced colonic inflammation and reduce the activation of the pro-inflammatory transcription factor nuclear factor kappa B (NF-κB) in rats. It has been proposed that black sorghum bran is able to protect against inflammation by altering the colon microbiota (Ritchie L. E., Carroll, Weeks, Rooney, & Turner, 2012), species diversity, species richness (Ritchie, et al., 2015) and the beneficial secondary metabolites produced by the microbiome (Ritchie, Sturino, Azcarate-Peril, & Turner, 2013).

Other fractions of sorghum have also been reported to reduce inflammation at both the cellular and the animal level. For example, aqueous and non-aqueous fraction of sorghum leaf sheaths reduced ROS formation by inflammatory polymorphonuclear (PMN) cells and the migration of these cells in response to the inflammatory chemoattractant leukotriene B4, with the ethanol fraction inducing a similar effect (Benson, et al., 2013). Other research demonstrated that a chloroform fraction of GS almost completely suppressed the lipopolysaccharide (LPS)-induced production of nitric oxide (NO), TNF-α and interleukin 6 (IL-6) (Hwang, et al., 2013). As a major constituent of GS, caffeoylglycolic acid methyl ester (CGME) was reported to exert anti-inflammatory effects by inducing heme oxygenases (HO)-1 expression via the nuclear factor-E2-related factor 2 (Nrf2)/heme oxygenase-1 pathway (Choo, et al., 2015). Caffeoylglycolic acid methyl ester (CGME) along with benzoic and cinnamic acid derivatives from GS also inhibited the production of NO and prostaglandin E_2 (PGE_2), IL-6 as well as the expression of iNOS, COX-2 and IL-6 in LPS-stimulated RAW 264.7 cells (Nguyen, et al., 2015) (Choo, et al., 2015).

B. Grain sorghum lipid profile and health benefits

The GS whole kernel contains high levels of lipid (3.0-4.9%), comparable or higher than many other cereal crops, such as corn (4.74%), wheat (1.71%), barley (1.16%) and rice (0.58%) (Hwang, Kim, & Weller, 2005). Serna-Saldivar and Rooney (1994) showed that the germ of GS contains the highest level of lipid (76.2%) followed by the endosperm (13.2%) and the pericarp (10.6%).

The lipid extract from the whole kernel, i.e., the lipid coating the surface of the kernel, has been analyzed by Carr et al. (2005) using thin layer chromatography (TLC, Figure 1). The lipid extract from whole kernel possesses a unique compositional profile, containing hydrocarbons, steryl esters, wax esters, aldehydes, alcohols, triacylglycerol, diacylglycerol, monoacylglycerol, free fatty acids and free sterols (Figure 2). This GS crude lipid (GS-CL) is composed of a wax and an oil fraction at a 2:1 or 3:1 basis (Lee, et al., 2014) (Wang, Weller, & Hwang, 2005). Hwang et al. (2002) showed that the wax fraction was composed of 46.3% fatty aldehydes, 7.5% fatty acids, 41.0% fatty alcohols, 0.7% hydrocarbons, 1.4% wax esters and steryl esters and 0.9% triacylglycerol. Alternatively triacylglycerols (~90%) were the most abundant compounds in the oil fraction as shown by Lee et al. (2014), but other important lipids were also present.

The health promoting potential of GS-CL has been mainly attributed to phytosterols and policosanols, which are located in the oil and wax fraction, respectively (Althwab, Carr, Weller, Dweikat, & Schlegel, 2015). In particular, evidence linking phytosterols to cholesterol lowering and anti-cancer benefits is increasing (Carr, Ash, & Brown, 2010) (Awad & Fink, 2000). Phytosterols present in the GS oil fraction exists as both free sterols and sterol esters (Singh, Moreau, & Hicks, 2003), with the predominant sterols being β-sitosterol, campesterol and stigmasterol (Leguizamón, Weller, Schlegel, & Carr, 2009). Phytosterol level ranges from 46 to 51 mg/100 g (Singh, Moreau, & Hicks, 2003) but varies depending on extraction method and the physical state of the sorghum material (Leguizamón, Weller, Schlegel, & Carr, 2009).

Policosanols have also been reported to improve blood lipid profile (Gouni-Berthold & Berthold, 2002) albeit other reports have disputed these claims (Lin, et al., 2004) (Dulin, Hatcher, Sasser, & Barringer, 2006) (Murphy, Saint, & Howe, 2008). These compounds account for 37-44% of the GS wax fraction (Hwang, Weller, Cuppett, & Hanna, 2004) with the major policosanols consisting of octacosanol (28:0) and triacontanol (30:0) followed by hexacosanol (26:0) and dotriacontanol (32:0) (Leguizamón, Weller, Schlegel, & Carr, 2009). Similar to the

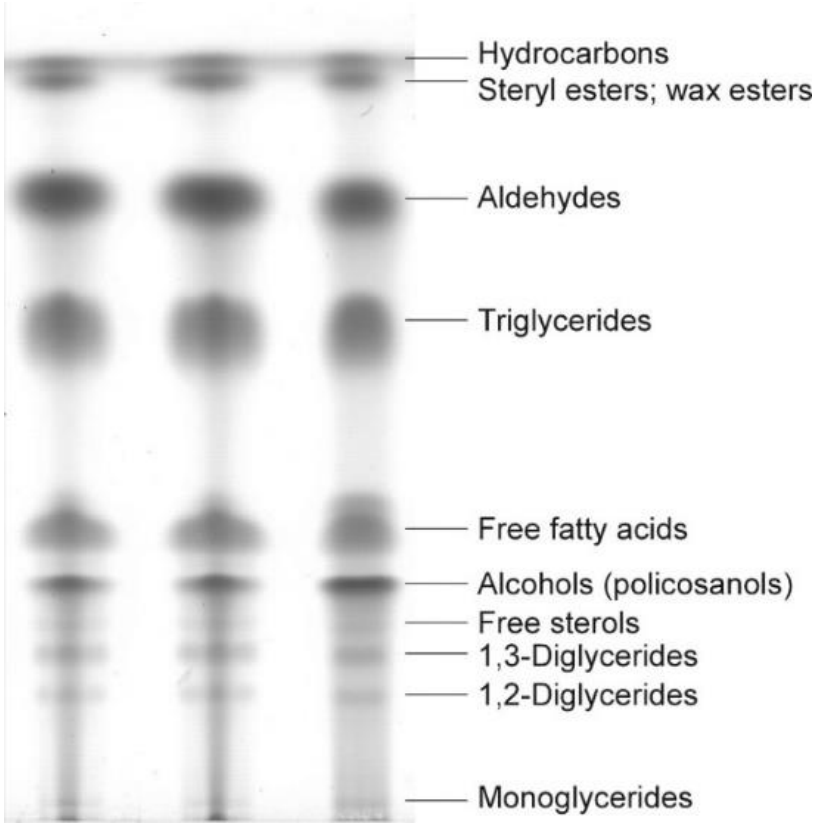

Figure 1 TLC analysis of white GS-CL (Carr, et al., 2005). TLC plate was developed in a solvent system of hexane: diethyl ether: acetic acid (85:15:2, by volume).

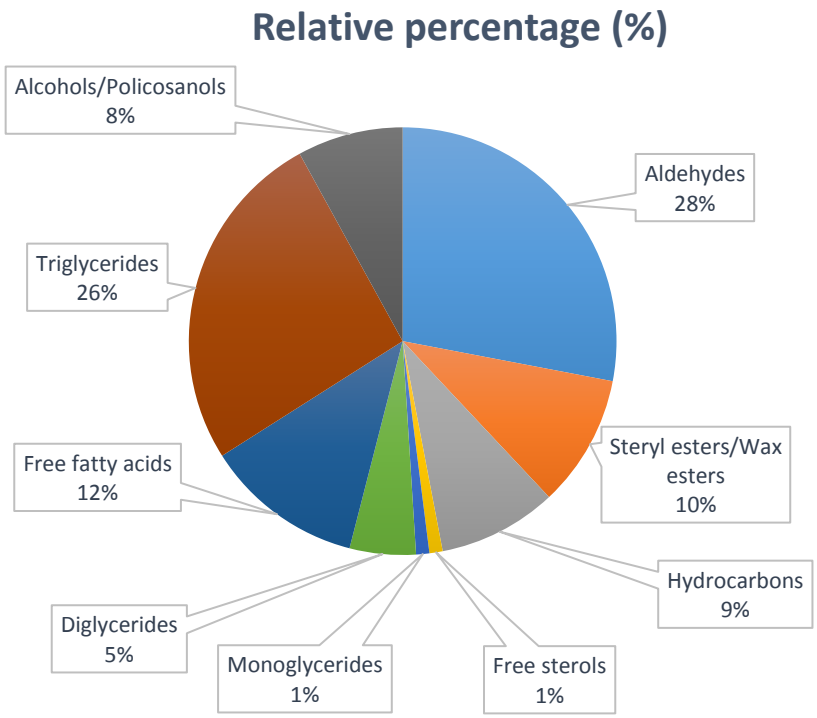

Figure 2 Illustration of lipid profile of white GS-CL (Carr, et al., 2005).

whole kernel phytosterols, the policosanol composition and quantity can differ due to the extraction method used, the physical form of GS (Leguizamón, Weller, Schlegel, & Carr, 2009) and the type of GS as established in this study.

i. Atherosclerosis

Carr et al. (2010) reviewed the positive impact of cholesterol lowering effect of phytosterols when consumed for therapeutical purposes, especially in terms of low density lipoprotein (LDL) cholesterol. Several researchers proposed that sorghum lipid extracts will improve plasma and liver lipid profile due to its high phytosterol content. To test this hypothesis, hamsters were fed a GS-CL supplemented (0.5, 1 and 5% w/w) fatty diet that was able to elevate both plasma and liver low density lipoprotein (LDL) cholesterol (Carr, et al., 2005). Plasma non-high density lipoprotein (HDL) levels decreased significantly when the animals were fed the 1 and 5% supplement, resulting in a reduction of 40 and 65%, respectively, compared to the animals fed the HF diet only. Plasma HDL cholesterol of the supplemented groups trended upward with the GS-CL supplements although not significantly. In addition, cholesterol absorption efficiencies of the hamsters consuming the 0.5, 1, and 5% GS-CL supplemented diets were reduced by 62.5%, 59.7% and 56.6%, respectively, compared to 67.2% presented by the HF group. The cholesterol lowering effect of GS-CL was thus attributed in part to the inhibition cholesterol absorption. Using the animal pellets from the above described project, Martínez et al. (2009) showed that the gut microbiota was altered and concluded that the cholesterol lowering effect of GS-CL could also be partially attributed to this effect.

On the other hand, Hoi et al. (2009) showed that GS dry distiller grain with soluble (DDGS) lipid fraction included into a HF diet also resulted in increased cholesterol excretion in a dose-dependent manner (0, 0.5, 1 and 5% of GS-DDGS), which correlated to decreased liver cholesterol concentration. Although plasma HDL levels were not affected by any of the doses, non-HDL did decrease but only for the 5% supplemented fatty diet (by 69%).

Lee et al. (2014) fractionated GS lipid obtained from whole kernel of white GS to the oil and wax extracts and showed that the phytosterols and policosanols remain in the oil fraction and in the wax fraction, respectively. Again using hamsters as the animal model, the oil supplemented (5%, w/w) into a fatty diet resulted in significantly lower non-HDL plasma (25% reduction) and liver esterified cholesterol (64% reduction). Alternatively, the wax supplement (5%, w/w) did not affect either plasma or liver cholesterol, but did increase excreted neutral sterols and bile acids. The researchers hypothesized that synergistic effects between oil and wax may be involved in the anti-atherosclerosis effect of as the GS-CL (Carr, et al., 2005) exerted greater benefits when compared to either the oil-wax fractionated results (Lee, et al., 2014). It must be noted however that the former study used diets that contained lower fat levels than the latter study. Still, the lipid fraction from the GS-DDGS (Hoi, et al., 2009) used a HF diet similar to that used in the original GS-CL study (Carr, et al., 2005), but the cholesterol lowering effects were much less. As such, synergism between the two fractions may play an important role in the protective properties of GS-CL.

The GS-CL could also exert its cholesterol lowering effect through the regulation of hepatic cholesterol metabolism, particularly effecting 3-hydroxy-3-methyl-glutaryl-coenzyme A (HMG-CoA) reductase, sterol regulatory element-binding protein (SREBP)-2 and fatty acid synthase. Kim, Kim & Park (2015) showed that all of these proteins were significantly downregulated whereas AMPK phosphorylation was considerably upregulated in hypercholesterolemia mice fed a GS supplement.

ii. Gastrointestinal regulation

Cholesterol homeostasis improvements in response to GS-CL consumption has been strongly associated with changes in gut microbiota based on a study of the gut microbiome of hamsters consuming GS-CL (Martínez, et al., 2009). As previously described, the study indicated that the regulating effects of GS-CL on hamster lipid profile, at least in part, act through the gut microbiota. These conclusions were based on the data showing a strong correlation between HDL

cholesterol levels and an increase in Bifidobacteria whereas a decrease in Coriobacteriaceae was significantly associated with non-HDL cholesterol (Martínez, et al., 2009). The hypothesis that dysregulated lipid profile could be attributed by the dysfunction of a single or several species of gut microbiota was thus proposed. To test this hypothesis, systematic gut microbiome sequencing and wide sampling from dyslipidemia population were needed. Therefore, in a latter study, Martínez et al. (2013) used plant sterol esters (PSE) to mimic phytosterols present in GS-CL. The results showed a prominent correlation between two species, Coriobacteriaceae and Erysipelotrichaceae, and the host fecal and biliary cholesterol excretion, which fit a bacterial inhibition model perfectly. The researchers further proposed that host cholesterol excretion modulated the microbiota through the antibacterial action of cholesterol, whereas PSE did not possess the inhibitory effect, which accounts for the different microbial composition between the groups (Martínez, et al., 2013).

II. Nutrient overload induces metabolic and energy switch

Exposure to excess nutrients and thereby energy is a modern phenomenon that has been caused by changes in dietary patterns and lifestyles. Although temporary nutrient excess can be accommodated and remediated by the inherent protective responses, chronic and persistent nutrient overload irreversibly disturbs metabolic homeostasis, leading to the gradual development of obesity (Zhang, et al., 2008). Indeed obesity has been linked to an array of metabolic disorders, including insulin resistance and type II diabetes (Lionetti, et al., 2009), cardiovascular diseases (Jia, Aroor, Martinez-Lemus, & Sowers, 2014) and even cancer (Taubes, 2012). The prevalence of obesity and its associated medical disorders has increased dramatically in the U.S. and throughout much of the world in the past decade (Jia, Aroor, Martinez-Lemus, & Sowers, 2014).

A. HF diets cause perturbations in energy metabolism

Of particular interest for our study, HF high cholesterol western diets induce prominent changes in energy metabolism. In order to cope with HF high cholesterol and low glucose, cells

switch to fatty acid β oxidation as the main energy source (Jiang , et al., 2013). Multiple researchers have conducted studies using HF high cholesterol fed animal models to understand the impacts of such a diet on human health. Zha et al. (2009) determined that a HF diet induces significant elevations in plasma fatty acids in a hamster model, whereas Boulangé et al. (2013) reported increased urine excretion of β oxidation intermediates in mice. Histopathological assessment also revealed excessive organ lipid accumulation (Jiang , et al., 2013) (An, et al., 2013). Examination of the urine showed higher circulating fatty acids and their metabolites indicating the upregulation in fatty acid breakdown through β oxidation. These results also imply fatty acid overflow through the mitochondria (Boulangé, et al., 2013). Excessive acetyl-CoA from mitochondrial fatty acid oxidation may then be stored by accumulating around and entering key organs, which has the potential of saturating the TCA cycle causing mitochondrial stress (Boulangé, et al., 2013). Furthermore, Boulangé et al. (2013) showed that tricarboxylic acid (TCA) cycle intermediates from succinyl-CoA to oxaloacetate (OAA) are significantly elevated in the urine of HF fed mice. An et al. (2013) also determined that HF intervention increases the levels of succinate and fumarate in rat liver. Chronic fatty acid overload in mitochondria leads to mitochondria overwork and impairment and, in turn, damaged energy metabolism.

As the intake of a HF western diet progresses, low glucose supply becomes more evident. Zha et al. (2009) and Guo et al. (2016) reported a reduction in plasma glucose level in a hamster model 12 to 24 weeks into HF feeding. Moreover, An (2013) showed a reduction in liver glucose and glycogen levels in a rat model. At the same time, circulating and liver alanine and lactate trended upward due to HF diet and low glucose supply to the muscles (An, et al., 2013). These results are most likely due to the lack of glucose as primary energy source, which is essential nutrient for many tissues that include central nerve system and red blood cells. The depletion of glucose thereby triggers the activation of several pathways employing non-carbohydrate substrate to synthesis glucose (Boulangé, et al., 2013).

Amino acid catabolism is significantly upregulated in animal models fed HF diets in an effort to generate more glucose. For example, levels of many amino acids, including methionine, phenylalanine, tyrosine, proline, tryptophan, glutamine, valine, lysine, glycine and histidine were reduced in the plasma of HF high cholesterol fed hamsters (Zha, et al., 2009) and HF fed rats (An, et al., 2013). Boulangé et al. (2013) also measured significant elevations of branched chain amino acid (BCAA) catabolic intermediates in urine excreted by HF fed mice, including leucine, isoleucine and valine intermediates. Coupled with higher levels of TCA intermediates from succinyl-CoA to OAA, the researchers concluded that the upregulated BCAA catabolism feeds into the TCA cycle as an anaplerosis source in order to produce glucose through gluconeogenesis (Boulangé, et al., 2013). An et al. (2013) also supported this conclusion with an exception that the HF diet group presented with significant reductions in urinary excretion of TCA intermediates including citrate, α-ketoglutarate (α-KG), succinate and fumarate. Additionally, Kowalski et al. (2015) performed an oral C^{13} glucose tolerance test on mice fed with a HF diet for 10 weeks. Compared to control mice (no fat included in the diet), the muscles of the HF diet mice resulted in a reduction of the C^{13} label for all the TCA cycle intermediates with the notable exception of citrate. These results were attributed to a gradual carbon dilution that were contributed by the alternative unlabeled carbon source entering the TCA cycle through multiple anaplerosis process, such as glutaminolysis and other amino acid catabolism.

As HF diet consumption proceeded to 42 weeks, circulating glucose and hepatic glucose and glycogen levels were restored via gluconeogenesis from amino acids and other non-carbohydrate substrates (Jiang , et al., 2013). Concurrently, urinary, hepatic and plasma alanine and lactate levels were reduced as reported by Guo et al. (2016) and Jiang et al. (2013). However, elevated glucose level remained in circulation without being taken up by cells due to a persistence HF intake fulfilling the role as main energy source. Ultimately, a HF diet could initiate many metabolic disorders, such as obesity, type II diabetes and atherosclerosis (Hotamisligil & Erbay, 2008) by initially eliciting stress responses.

B. HF diets initiate intestinal stress via various mechanisms

Epidemiological studies have shown that a HF western style diet increases the risk of inflammatory bowel diseases (Teixeira, et al., 2011) (Kim, Gu, Lee, Joh, & Kim, 2012). As reported by Kim et al. (2010), a HF diet increased the susceptibility of mice to DSS-induced inflammation and exacerbated the severity of DSS-induced colitis. Increased macrophage not only infiltrated the sub-epithelial region of lamina propria but also at the base of crypts and in the sub-mucosal layer (Erdelyi, et al., 2009) (Cheng, et al., 2016) (Kim, et al., 2010). Moreover, the HF diet induced the expression of the pro-inflammatory cytokines (TNF-α, IL-1β, and IL-6) and the activated pro-inflammatory enzymes and proteins such as NF-κB, iNOS, myeloperoxidase (MPO) and monocyte chemoattractant protein (MCP)-1 (Kim, Gu, Lee, Joh, & Kim, 2012) (Bastie, et al., 2012).

Kim et al. (2012) showed that mice fed a HF diet exhibited higher endotoxin levels in both plasma and fecal samples, indicating the progression of localized intestinal inflammation to systemic inflammation. High circulating endotoxin levels also indicate increased intestinal permeability. This research was supported by Murakami et al. (2016) and Kim et al. (2012) who both showed reduced expression of tight junction proteins, markers for intestinal hyperpermeability in the colon of mice fed a HF diet (Murakami, Tanabe, & Suzuki, 2016). Intestinal permeability has been associated with gut microbiota dysregulation. For example, Kim et al. (2012) showed that HF diet dysregulates gut microbiota by increasing the ratio between *Firmicutes* and *Bacteriodetes*, and also induces the growth of *Enterobacteriaceae* in a mice model. Shen et al. (2014) also reported that mice fed with HF diet have greater abundance of 3 types of sulfidogenic bacteria in colonic mucosa, resulting in the production of the pro-inflammatory compound, hydrogen sulfide (Carbonero, Benefiel, Alizadeh-Ghamsari, & Gaskins, 2012).

In addition to local and systemic inflammation, Erdelyi et al. (2009) demonstrated that the HF diet induces oxidative stress in colon, as genes involved in oxidative stress responses were unregulated, including Nrf2, a redox sensitive transcription factor. Moreover, metabolic profiling of colonic redox active compounds showed that HF feeding significantly reduces cysteine: cystine ratio, providing further proof of colonic oxidative stress (Erdelyi, et al., 2009), which if left unchecked can lead to chronic inflammation and associated diseases.

III. Metabolomics research on bioactive food ingredients

A. Metabolomics

By definition, the metabolome is a "snapshot" of the entire complement of metabolites produced at any given point in time by a biological system. It is therefore the goal of metabolomics to describe, both qualitatively and quantitatively, the metabolome. Metabolomics can thus monitor changes of the complete set of metabolites in and derived from an organism, the end products of gene expression and/or in response to environmental changes (van der Werf & Venema, 2001). Metabolomics is the most recent addition to the applied genomics technologies, or the 'omics', that include genomics, transcriptomics and proteomics. Although the least well defined of the 'omics' technology, metabolomics provides multiple attributes in terms of understanding a complex system. Firstly, the number of metabolites (~2,500) is more than an order of magnitude lower than the 30,000 to 40,000 genes in the human genome, making it a simpler screening tool (Kell, 2006). Secondly, as metabolic pathways between species and organisms are highly conserved (Nikolaev, Burgard, & Maranas, 2005) (Ravasz, Somera, Mongru, Oltvai, & Barabási, 2002), metabolomics allows the use of biological models to reflect biochemical changes in response to external stimuli (Weljie, Dowlatabadi, Miller, Vogel, & Jirik, 2007). And thirdly, as the final downstream outcome of the genome, transcriptome and proteome, the metabolome reflects phenotype or function (Weljie, Dowlatabadi, Miller, Vogel, & Jirik, 2007). In other words, if the blueprint of any biological system is represented by the genome,

then its function is expressed by its metabolome. Therefore, metabolomics is able to provide a metabolic snapshot of an organism by bridging the genotype to phenotype gap.

The main challenges of metabolomic based research are the heterogeneity of the molecules, low dynamic range of analytical techniques, limited through-put of the instruments and the lack of validated extraction protocols. To date, it is impossible to analyze multiple classes of metabolites with a single analytical method. Selection of appropriate metabolomic analytical techniques is usually a compromise between high-throughput, selectivity and sensitivity requirements. To achieve a comprehensive and accurate understanding of a metabolome, at least two or more analytical techniques are needed. The most commonly employed analytical methods include gas chromatography (GS), high performance liquid chromatography (HPLC), capillary electrophoresis (CE), nuclear magnetic resonance (NMR), and mass spectrometry (MS) (Gries, 2008).

Two approaches are typically cited to conduct a metabolomics study, i.e., metabolic profiling and metabolic fingerprinting, which simplifies the study of the metabolome. Metabolic profiling refers to the analysis of a set of preselected metabolites with the goal of identifying and quantitating each metabolite. However, this strategy limits the detection to molecules with specific characteristics, such as similar chemistries (organic acids versus amino acids,) pathways of origin (tricarboxylic acid vs eicosanoid pathway), biological relevance (specific metabolic biomarkers) and / or physiological interactions (Dettmer & Hammock, 2004). As such metabolic profiling provides precise and accurate changes to a wide array of key metabolites in response to various genetic or environmental stimuli. When key metabolites can be analyzed simultaneously, metabolic profiling can be equally or even more powerful as a global metabolomics, or metabolic fingerprinting. The latter approach does not identify specific metabolites but rather compares changes in patterns of metabolic responses to environmental stimulations or genetic perturbations (Dettmer & Hammock, 2004). The entire data set or sub-set can then be analyzed by pattern recognition and related multivariate statistical approaches to determine if the responses are

significant between samples. Depending on the objective of a study, researchers are currently applying one or both approaches (Lee, 2013).

B. Metabolomics as a tool to study the effects of dietary bioactive agents

Metabolomics has been employed to investigate the health benefits of bioactive food ingredients although these studies remain limited. Nevertheless, Zhou et al. (2015) applied metabolic profiling on the urine of a hyperlipidemia rat model by using ultra-performance liquid chromatography (UPLC) coupled with electrospray ionization quadruple time-of-flight mass spectrometry (ESI-QTOF-MS) to investigate the regulatory effect of mangiferin. The ensuing data were then analyzed with principle component analysis (PCA) and orthogonal partial least-squares discriminant analysis (OPLS-DA) to visualize the metabolic trajectory as a means to discover potential biomarkers affected by a HF diet and mangiferin administration (Zhou, et al., 2015). Li et al. (2015) employed proton nuclear magnetic resonance (^{1}H NMR) coupled with mass spectrometry to conduct metabolomic profiling on the urine of hyperlipidemia mice fed a diet supplemented with curcumin. By combining the ‘omics’ with statistical analysis to study nutraceutical intervention, the researchers were able to identify more natural substances that may have medical values. Such applications provided the foundation for this research.

2. Objective and specific aims

The health promoting properties of most dietary components have been primarily studied using isolated components despite emerging but limited research showing that whole food or complex rich extracts impart greater health benefits than the sum of the individual components (Junio, et al., 2011). Moreover, the metabolic mechanisms that recognize and respond to such molecules and thereby promote a healthy state remain largely unknown. The *objective of this project* was to determine the ability of GS-CL (rich in both health benefiting phytosterols and policosanols) to protect energy pathways and the short chain fatty acid (SCFA) profile produced by gut microbiome thus mitigate intestinal stress caused by a HF diet, which if left unchecked can lead to hypoxia or inflammation, that in turn can progress into other chronic conditions. Considering that the surface of GS contains a complex matrix of lipids, including phenols for tannin containing sorghums, the central hypothesis for this project is that this richly diverse extract is able to protect the following pathways, glycolysis, TCA, pentose phosphate pathway (PPP), and amino acids (i.e., the precursors of many energy metabolites) against modulation caused by a HF diet. Moreover, the GS-CL is expected to prevent the HF diet from interfere the production of SCFA produced by the gut microbiome. This hypothesis was tested by completing the following specific aims.

Specific Aim 1: *To determine the ability of different dosages of red GS-CL (1,3 and 5%) to prevent intestinal stress caused by a HF diet by monitoring key energy pathways (carbohydrate, amino acid and nucleotide metabolism) by using a hamster model and metabolic profiling approaches.* The working hypothesis for this aim is that the red GS-CL will provide a protective response against HF induced energy modulation in intestine but the degree will be dependent on GS-CL dosages.

Specific Aim 2: *To determine the ability of different dosages of red GS-CL (1,3 and 5%) to prevent the impact of HF diet on the production and profile of SCFA in large intestine.* The

working hypothesis for this aim is that the red GS-CL will provide a protective response against the inhibitory effect of HF diet on SCFA profile produced by the gut microbiome.

Specific Aim 3: *To characterize red GS-CL in terms of its chemical compositions.* The accessed need for this aim is that such information was required to ultimately determine the components responsible for protecting against intestinal stress.

3. Material and methods

I. Specific Aim 1 and 2: Metabolic actions of fatty diet without and with different doses (1, 3, 5%) red grain sorghum crude lipid on key energy pathways and SCFA profile

A. Grain sorghum crude lipid extraction

The GS-CL was prepared with food grade dark red high tannin GS whole kernel (a germplasm line from the Texas AES-USDA sorghum conversion program) provided by Dr. Ismail Dweikat (University of Nebraska-Lincoln) and Nu Life Market, Kansas, grown and harvested in 2014. The GS-CL was extracted from the surface of red GS by refluxing, previously described by Leguizamón et al. (2009). Briefly, whole kernel red GS (1 kg) was refluxed with hexane (1 L) for 30 min at a temperature slightly below 60 °C in a three-neck round bottom flask connected to a condenser. The mixture was cooled to room temperature and then passed through two layers of coffee filter and a Whatman No. 2 filter under vacuum. The solvent was evaporated from the GS extract using a rotavapor. The residue GS-CL was collected and stored at -18°C until use.

B. Diet and animal care

Five different diets were prepared based on the AIN-93M purified diet, which consisted of a negative control (low fat), an high fat (HF) positive diet and three HF diets supplemented with either 1.0, 3.0, and 5.0% (w/w) GS-CL (Table 1). For the HF diets, coconut oil, cholesterol and GS-CL supplements were added at the expense of cornstarch.

Fifty five male Syrian hamsters (Charles River, Wilmington, MA), age 9 weeks with body weight ranging from 110 to 120 g, were used for this study. The hamsters were randomly assigned to the five experimental diets (n=11) to ensure a similar average weight among the groups. Each hamster was housed individually in polycarbonate cage with wood chip bedding in

a controlled environment of 25 °C with a 12 h light-dark cycle, and had free access to water and food. The animals were maintained on their assigned diet for 4 weeks, and their food intake was recorded on a weekly basis. The bedding was also changed weekly, whereas the body weight of each hamster was measured at baseline and at the end of the study. Food was removed 14 h before CO_2 asphyxiation to achieve overnight fasting. The large intestine was collected, immediately frozen with dry ice and stored at -80 °C until analyzed. All experimental procedures were approved by the Institutional Animal Care and Use Committee at the University of Nebraska.

C. Extraction of targeted metabolites

Metabolite extraction was initiated by grinding the frozen large intestinal tissue in dry ice until a fine powder was produced. Approximately 120 mg of the ground tissue was weighed in a 1 mL glass homogenizer followed by the addition of 1 mL ice-cold nanopure water. The tissue was then homogenized while maintained in flaked ice until no large tissue pieces were visible. The homogenate was then centrifuged with a Beckman GS-6R centrifuge at 4°C for 30 min, which completed pelleted the solid material. The supernatant was collected and passed through a EMD Millipore Amicon centrifugal filter unit 10 KDa to achieve a clear, protein-free metabolite extract. The extract was concentrated with a Labconco CentriVap concentrator to a total volume of approximately 100 µL (Figure 3).

D. Analysis of tissue extracts

The eight glycolysis intermediates and two pentose phosphate pathway intermediates were analyzed using a LC-ESI-MRM-MS. Samples were evaporated to dryness using a Speed-vac concentrator (Thermo Savant Instruments, USA) at 4 °C. The pellets were re-dissolved in 50 µL of nanopure water and vialed prior to injection on the LC system. The HPLC (Agilent 1200 series, Santa Clara, CA) separation was achieved using an XBridge Amide column (2.1 × 100 mm, 3.5 µm) (Waters Millipore, Milford, MA). The mobile phase consisted of 20 mM

Table 1 Composition of five hamster diets.

Food Component*	Control	HF[1]	HF + 1% GS-CL[2]	HF + 3% GS-CL[2]	HF + 5% GS-CL[2]
Cornstarch	455.7	353.7	343.7	323.7	303.7
Dextrinized cornstarch	155.0	155.0	155.0	155.0	155.0
Casein	140.0	140.0	140.0	140.0	140.0
Sucrose	100.0	100.0	100.0	100.0	100.0
Coconut oil	---	100.0	100.0	100.0	100.0
Soybean oil	50.0	50.0	50.0	50.0	50.0
Insoluble fiber (cellulose)	40.0	40.0	40.0	40.0	40.0
Soluble fiber (guar gum)	10.0	10.0	10.0	10.0	10.0
GS-CL	---	---	10.0	30.0	50.0
Cholesterol	---	2	2	2	2
AIN-93 mineral mix	35.0	35.0	35.0	35.0	35.0
AIN-93 vitamin mix	10.0	10.0	10.0	10.0	10.0
L-Cysteine	1.8	1.8	1.8	1.8	1.8
Choline bitartrate	2.5	2.5	2.5	2.5	2.5

* Dyets, Inc. Bethlehem, PA;
[1]HF diet contained extra coconut oil and cholesterol at concentrations of 10% and 0.2%, respectively, at the expense of cornstarch;
[2]GS-CL were added at 1.0, 3.0 and 5.0% at the expense of cornstarch.

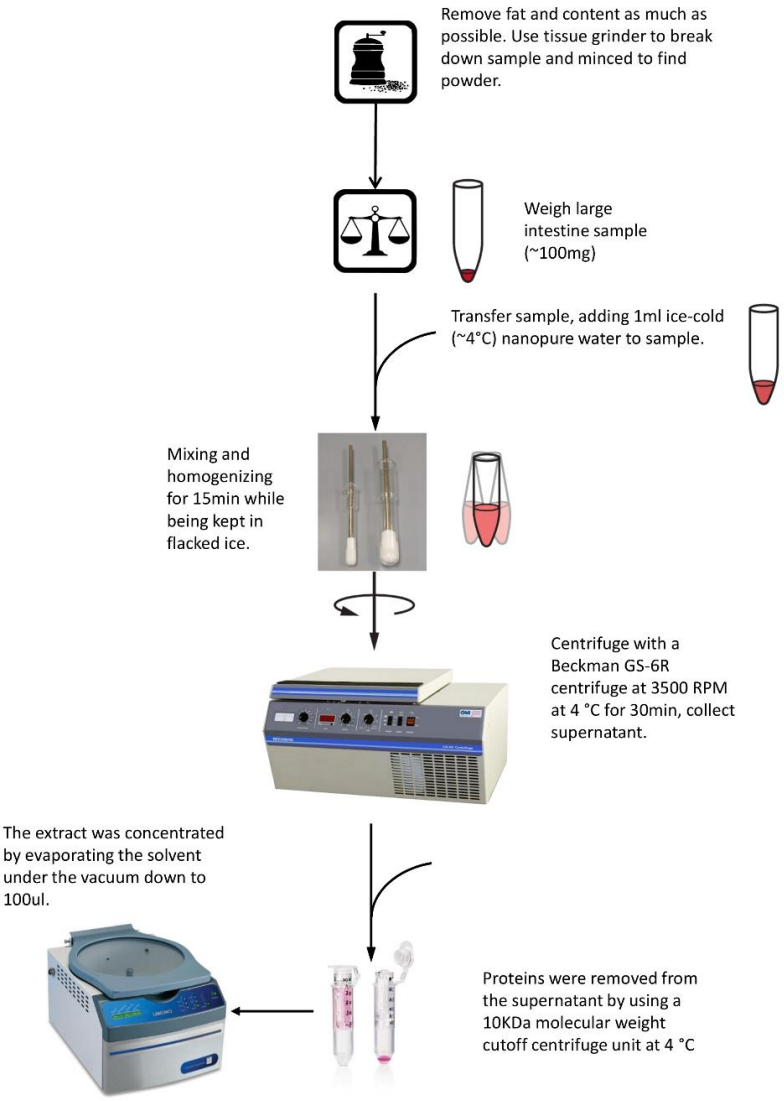

Figure 3 The extraction of tissue metabolites.

ammonium hydroxide and 20 mM ammonium acetate in nanopure water (A) and LC-Grade Acetonitrile (B). The gradient began at 5% A and 95% B for 3 min, then to 95% B over 10 column volumes, 95% B over 5 column volumes and finally 5% A over 10 column volumes; all steps at a flow rate of 0.5 mL/min. The eluent of the column was fed into the electrospray ion (ESI) ion source operating in negative ionization mode at a voltage of -4500 V, at a temperature of 500 °C and with source gasses at 60 L/min (GS1 and GS2). Multiple reaction monitoring (MRM) was employed for metabolite detection and quantification on a Sciex 4000QTrap (Framingham, MA). A single precursor and single fragment m/z values were paired for the detection of each metabolite. External standards at 10 ug/mL were used for calibration (Sigma-Aldrich, St.Louis, MO). All data was normalized according to tissue weight, and each metabolite was expressed as mean +/- standard error of the mean (µg/g) of eleven biological replica.

Amino acids were analyzed using EZ: faast™ amino acid analysis kit (Phenomenex Ltd. Germany) as per manufacturer's instructions. This analysis consisted of a solid phase extraction step followed by a derivatization and a liquid/liquid extraction, and the derivatized samples were quickly analyzed by gas chromatography with FID detection. More specifically, the solid phase extraction was performed via a sorbent packed tip that binds amino acids while allowing interfering compounds to pass through the column. The amino acids bound to the sorbent were then released with sodium hydroxide, 3-picoline and N-propanol. The sample mixture was allowed to incubate at room temperature during derivatization, which was accomplished with the above mentioned reagent. After a clear separation occurred between the organic and aqueous phases, the upper organic phase containing the derivatized amino acids was collected and analyzed on an Agilent 7820A GC instrument with a flame ionization detector (FID) detector. The amino acids present in the extracts were resolved, identified and quantified with a 10m × 0.25mm Zebron™ EZ-AAA amino acid GC column under the following conditions: initial oven temperature 110 °C, rising to 320 °C at 32 °C/min with the injector temperature set at 250 °C. The carrier gas was helium adjusted to a split ratio of 15:1. Each amino acid was quantified

against an internal standard (Norvaline). All data was normalized according to tissue weight and each amino acid was expressed as mean +/- standard error of the mean (µg/g) of eleven biological replica.

The remaining metabolites listed (Table 2) were analyzed with Beckman P/ACE MDQ capillary electrophoresis system (Beckman Coulter, USA) interfaced to a 67 cm long Agilent bare fused silica capillary (i.d. 50 µm) and a 200 nm UV filter. A 250mM sodium phosphate buffer (pH 6.0) containing 0.1 mM hexadecyltrimethylammonium bromide (CTAB) and 5% methanol served as background electrolytes (BGE) and the samples were injected onto the capillary using a pressure of o.5 psi for 5 sec, and the metabolites were separated at 25 °C and 10 KV. For all the CE assays, the capillary was preconditioned regeneration solution (0.1 N NaOH, Beckman Coulter, USA) for 2 min and running buffer for 2 min. After each run, the capillary was cleaned by rinsing with 1 M HCl for 2 min, capillary regeneration solution for 5 min and nanopure water for 2 min. All solutions and samples were filtered by a 0.45 µm filter unit before injected to the capillary. Standard curves for each metabolite were constructed with a cocktail containing external standards. The sample analyte peaks were identified by both retention time and standard spikes. System control, data acquisition, and data analysis were performed with a Beckman 32 Karat workstation. All data was normalized according to tissue weight and each metabolite was expressed as mean +/- standard error of the mean (µmol/g) of eleven biological replica.

II. Specific Aim 3: Characterization of grain sorghum (*sorghum bicolor*) crude lipid

The simple lipid profile was acquired using thin layer chromatography (TLC), as described by White et al. (1998). A cocktail of standards containing monoacylglycerols, 1,2-diacylglycerols, 1,3-diacylglycerols, triacylglycerols, fatty acid methyl esters, D-α-tocopherol acetate, three polyoxyethlenesorbitan monooleate and octacosanol was prepared. Approximately

Table 2 Metabolites of targeted metabolomic profiling.

	Metabolites	Analytical method
Glycolysis	Glucose-1-phosphate	MS
	Glucose-6-phosphate	MS
	Fructose-6-phosphate	MS
	Fructose-1,6-phosphate	MS
	Dihydroxyacetone phosphate	MS
	Glyceraldehyde-3-phosphate	MS
	Glycerol-3-phosphate	MS
	Glycerate-3-phosphate	MS
	Phosphenolpyruvate	CE
	Pyruvate	CE
Pentose phosphate pathway	Ribose-5-phosphate	MS
	Ribose	MS
TCA cycle	Acetyl-CoA	CE
	Citrate	CE
	α-ketoglutarate	CE
	Succinate	CE
	Malate[3]	CE
	Fumarate	CE
Coenzymes	NAD+	CE
	NADH	CE
	NADP+	CE
	NADPH	CE
	GSH	CE
	GSSG[4]	CE
Organic acids	Oxalate[2]	CE
	Formate	CE
	Malonate[1]	CE
	Acetate	CE
	Propionate	CE
	Butyrate[1]	CE
	Lactate[1]	CE

Amino acids	Alanine	GC
	Sarcrosine	GC
	Glycine	GC
	α-aminobutyric	GC
	Valine	GC
	Leucine	GC
	Isoleucine	GC
	Threonine	GC
	Serine	GC
	Proline	GC
	Asparagine	GC
	Aspartic acid	GC
	Methionine	GC
	Hydroxyproline	GC
	Glutamic acid	GC
	Phenylalanine	GC
	Glutamine	GC
	Ornithine	GC
	Lysine	GC
	Histidine	GC
	Tyrosine	GC
	Tryptophan	GC
	Cysteine	GC
Nucleotides	ATP	CE
	ADP	CE
	AMP	CE
	GTP	CE
	GDP	CE
	GMP	CE

All amino acid standards come from EZ: faast™ kit, the rest of standards were purchased from Sigma-Aldrich, except for the following:
[1] Standard purchased from Alfa Aesar;
[2] Standard purchased from Fisher chemical;
[3] Standard purchased from MP Biomedicals, LLC;
[4] Standard purchased from Fluka.

25 mg of the extracted GS-CL was suspended in 1 mL of chloroform to a final concentration of 20 mg/mL. The GS-CL was completely dissolved by heating to 60°C. The sample and standard was spotted on a 10 × 20 cm silica gel 60 plate using 10 µL aliquots. The plate was then placed in a resolving chamber containing hexane, diethyl ether and acetic acid (85:15:2, by volume) until the solvent had eluted near the top of the plate. The plate was removed and submerged briefly in 10% cupric sulfate, 8% phosphoric acid solution and air-dried in a chemical fume hood. Bands were visualized by charring the dried plate in an oven adjusted to165 °C for 10 min.

The GS-CL fatty acid profile was analyzed with a Agilent 7820A gas chromatograph (GC) system interfaced to a FID, and the resolution method used was based on the procedure previously described by Metcalfe et al. (1966). Briefly, a sample of GS-CL (0.05 g) was derivatized to volatile fatty acid methyl esters (FAMEs) by mixing with 2 mL of 14% boron trifluoride in methanol and heating at 100 °C for 5 min. After cooling to room temperature, the FAME were extracted with 1:2 hexane and water (v/v) by centrifugation until a well-defined pellet had formed. The FAMEs-containing hexane layer was analyzed using a GC DB-Wax column (30 m × 0.25 mm, J&W Scientific) under the following conditions: initial oven temperature was 185 °C for 12 min, increased to 210 °C at 10 °C /min, held for 1 min using a FID temperature of 250 °C. Helium served as the carrier, which was set at a split ratio of 10:1. Fatty acid levels were reported as relative percent of 100% crude lipid.

Quantification of phytosterols and policosanols present in the GS-CL was achieved by GC (Agilent 7820A GC system) interfaced to a FID. Based on the procedure described by Leguizamón et al. (2009), a GS-CL sample (0.02 g) was mixed with the internal standards, 0.1 mg 5α-cholestane and 0.1 mg policosanol heptacosanol (C_{27}). The mixture was saponified with 1 M methanolic potassium hydroxide at 50 °C for 1 h with occasional agitation. Non-saponifiable lipids were separated by adding 1 mL of deionized water and 3 mL of hexane to the mixture. The hexane phase was separated by centrifuging at 3000×g for 5 min and evaporated under nitrogen at 50 °C. The dried lipids were derivatized by reacting with 100 µL pyridine for 30 min followed

by the addition of 50 µL Sylon BTZ (Supelco, Bellefonte, PA, USA) at room temperature. Each sample was analyzed with a 0.32 mm × 30 m DB-5 capillary column (J&W Scientific, Folsom, CA, USA) under the following conditions: initial oven temperature was 100 °C, rising to 300 °C at 5 °C/min with the injector and FID temperature set at 270 °C and 300 °C, respectively. Helium served as the carrier, which was adjusted to a split ratio of 50:1. External phytosterols were used to identify and quantitate the individual phytosterols that included stigmasterol, sito-sterol and campesterol. Each type of policosanol and sterol were expressed as the mean +/- standard deviation (µg/g of lipid extract) of triplicate analyses.

Tocopherols present in the GS-CL extract were determined following a colorimetric method described by Wong, Timms and Goh (1988) with minor modification. A sample (200 mg) was weighed into a 10 mL volumetric flask and 5 mL hexane: isopropanol (3:2, v/v) was then added. The GS-CL was allowed to dissolve in this solvent by occasionally agitating the sample at room temperature followed by adding 3 mL of 0.07% 2,2'-bipyridine in 95% ethanol and 0.5 mL 0.2% ferric chloride in 95% ethanol sequentially. The sample was bought to a final volume of 10 mL with 95% ethanol, and absorption was measured with a Beckman Coulter DU800 spectrophotometer at 520 nm. An external calibration curves was constructed using the same method but employing the standard, α-tocopherol. Tocopherol levels in the sample were calculated as the mean +/- standard deviation mg equivalents of α-tocopherol per g of crude lipid of triplicate analyses.

Carotenoid levels were determined following a colorimetric method described by Lichtenthaler and Buschmann (2001). A sample of GS-CL(200 mg) was weighed into a screw cap tube followed by the addition of 1.6 mL methanol: water (94:6, v/v). The mixture was sonicated for 30 min in 45-50 °C water bath, and then centrifuged for approximately 5 min to collect a clear supernatant. After previous steps were repeated two additional times 1.2 mL of methanol: water (94:6, v/v) were added to the sample to a final volume 6 mL. The solution was then centrifuged until clear supernatant was obtained, and the absorbance was measured with a

Beckman Coulter DU800 spectrophotometer at 470, 853 and 666 nm. The concentration of carotenoid was calculated as µg per g GS-CL by the following equations:

$$Chlorophyll\ A\ (\mu g/ml) = 15.65A_{666} - 7.34A_{653}$$

$$Chlorophyll\ B\ (\mu g/ml) = 27.05A_{653} - 11.21A_{666}$$

$$Carotenoids\ concentration\ (\mu g/ml) = (1000A_{470} - 2.86)\times(chlorophyll\ A - 129.2)\times chlorophyll\ B/245.$$

This test was completed in triplicate and the carotenoid levels were expressed as the mean +/- standard deviation (µg/g of lipid extract).

Lastly, tannin levels were determined by following a liquid-liquid extraction method described by Fuentes et al. (2012). A sample (2.5 g) of GS-CL was dissolved in 5 mL of hexane followed by the addition of 3 mL methanol:water (60:40, v/v). The mixture was centrifuged to achieve a clear phase separation. The methanol phase was collected, and the liquid/liquid extraction was repeated an additional time. The methanol phases from the two extractions were combined for tannin detection following a colorimetric method described by Bhat, Sridhar, and Tomita-Yokotani (2007). The methanol extract (1 mL) was combined with 5 mL of 4% vanillin in methanol and 8% HCL in methanol (1:1). After 20 min of incubation at room temperature, the absorbance was measured at 500 nm. Tannin levels were determined by constructing a calibration curve using catechin as an external standard. The tannin content was expressed as the mean +/- standard deviation of mg equivalents of catechin per g GS-CL of triplicate analysis.

III. Statistical Analysis

Univariate comparisons between control and HF groups were performed in R using non-parametric Kruskal-Wallis test. Pairwise comparisons among the five treatment groups were performed in GraphPad Prism version 7 (GraphPad Software, La Jolla CA, USA) using one-way ANOVA followed by Tukey's multiple comparison after confirming normal distribution in R. To compare metabolic changes among the groups, multivariate analysis was conducted, including

partial least squares-Discrimination analysis (PLS-DA) and orthogonal-PLS-DAs which were performed with MetaboAnalyst 3.0 (www.metaboanalyst.ca) and SIMCA-P^+ 12.0 software (Umetrics; Sweden), respectively.

4. Results and discussion

The health promoting properties of GS-CL reported to date has mainly focused on cholesterol management (Carr, et al., 2005) (Lee, et al., 2014) (Hoi, et al., 2009) with fewer reports on its role in modulating the intestinal microbiota (Martínez, et al., 2009) (Lee, 2013). Despite these established benefits, a critical gap in information remains on the impact of GS-CL on cells or tissues at the "omics" level, with an exception of a study performed by Lee (2013). In the latter research, metabolomic profiling was performed on both the liver and large intestine collected from hamsters fed HF diets supplemented with either 5% white GS oil or wax. The supplemented diets compensated for the changes caused by a HF diet to a large degree in large intestine, but the liver metabolome was affected only minimally (Lee, 2013). In the current study, metabolites of key energy pathways were profiled more extensively to achieve a comprehensive understanding of the mode of action behind this compensation in large intestine, and to determine if different lines of sorghum provided different benefits. Furthermore, the SCFA produced by the gut microbiome were also analyzed to determine whether the red GS-CL were able to mitigate the effects of HF on the microbiome. Lastly, the GS-CL was thoroughly characterized to provide information of the possible component(s) responsible for these effects.

I. Animal body weight and food intake

Baseline body weight of the hamsters were not significantly different among groups (117.13 ± 0.08 g). After the four week feeding study, each group gained weight (129.2 ± 2.7 g) with an average gain of 13.4 ± 2.1 g, which was not statistically different among the groups. In addition, food intake throughout the study remained constant for all groups (9.8 ± 0.5 g/day), showing that the supplemented diets were palatable.

II. Specific aim 1: Metabolic actions of HF diet without and with different doses (1, 3 and 5%) of red GS-CL on key energy pathways

A. The effect of a HF diet on cellular central carbon metabolism

i. Effect of HF diet on cellular energy production and redox balance

Cellular energy status is reflected by the index "energy charge", first defined by Atkinson and Walton (1967), which is shown below.

$$Energy\ charge = \frac{[ATP] + \frac{1}{2}[ADP]}{[ATP] + [ADP] + [AMP]}$$

When applied to the nucleotide data obtained from the intestinal analysis of both the control and HF groups, a significantly lower energy level (0.062 ± 0.004) was detected in the HF group than that of the control (0.297 ± 0.102) (Figure 4). These results thus confirm that a HF diet affects the ability of intestinal cells to generate energy, creating a hypoxic stress relative to a low fat diet.

The HF diet consumed by the model system may have impaired their ability to generate energy by multiple mechanisms. First, the HF diet contained 10% more fat and less starch than that of the control diet (Table 1). Excessive fatty acids may have accumulated quickly in mitochondria for β oxidation, thereby over-stressing the organelle. This stress may have resulted in possible damages to the electron transport chain (ETC) (Boulangé, et al., 2013), and/or impairment to its ability to recycle NADH to NAD+. As is shown in Figure 5, the HF group presented with significantly lower NAD+ (4.05 ± 0.41nmol/g) when compared to control group (6.19 ± 0.65 nmol/g). The NAD/NADH ratio corresponding to the HF group (0.343 ± 0.029) was also much lower than that of the control group (0.488 ± 0.080). Similar to these results, several studies have shown that under excessive substrate availability, whether the substrate was glucose, lipid or amino acids, NAD+ decreased in skeletal muscle, liver and heart (Gumaa, McLean, & Greenbaum, 1971) (McGarry & Dobbins, 1999) (Vettor, et al., 1997). As the carrier of electrons generated from glycolysis and the TCA, the lower NAD+ and NAD/NADH ratio obtained from

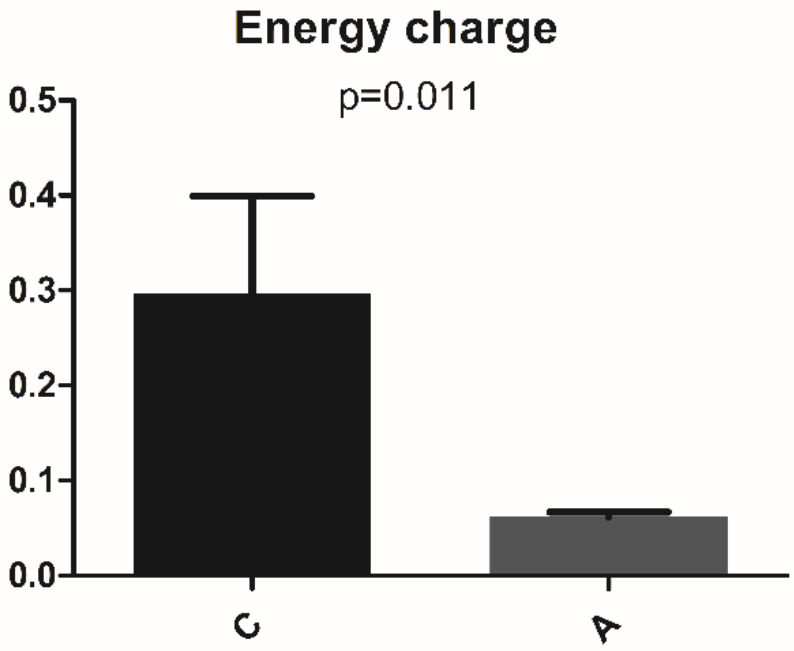

Figure 4 Energy charge for control and HF groups. Values are shown as the means ± SEM, n=11. Statistical differences were evaluated using non-parametric Kruskal-Wallis test.

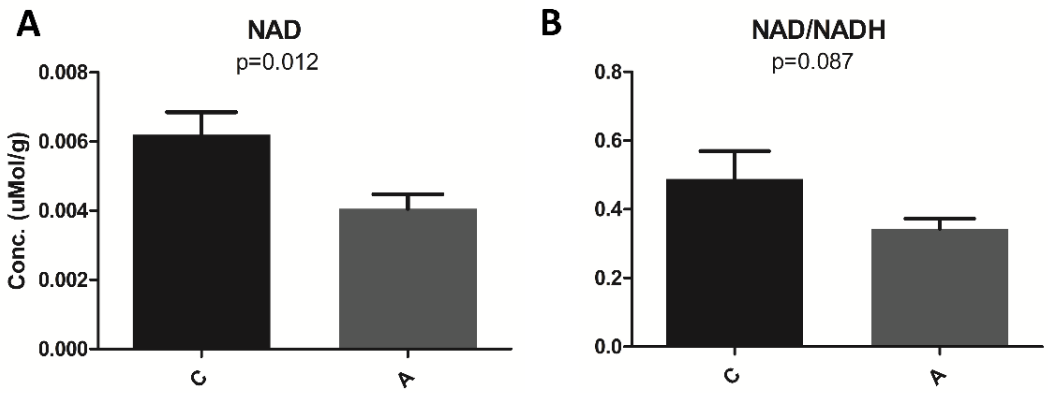

Figure 5 NAD+ and NAD/NADH ratio of control and HF groups. Values are shown as the means ± SEM, n=11. Statistical differences were evaluated using non-parametric Kruskal-Wallis test.

our studies denote a reduction in the ability of the intestinal cells to generate energy by disrupting cellular redox balance and causing oxidative stress (Rosca, et al., 2012).

This hypothesis was tested by monitoring glutathione in both its reduced (GSH) and oxidized forms (GSSG) as GSH is considered one of the most important free radical scavengers. The ratio of GSH/GSSG has thus been employed as a marker of cellular redox balance and oxidative stress (Zitka, et al., 2012). For the HF group, the GSH/GSSG ratio and GSH level were 0.336 ± 0.026 and 0.015 ± 0.000 µMol/g respectively, trending lower than the 0.523 ± 0.108 and 0.018 ± 0.002 µMol/g of the control group (Figure 6). Similarly, Ajiboye et al. (2016) also reported a decrease in GSH and GSH/GSSG ratio in the livers of HF fed rats.

ii. Effect of HF diet on central carbon metabolism

Glucose is the primary energy source for many organs, including the large intestine. Therefore, when fat is present in the diet at high levels, the cells are forced to use fatty acids as an energy income to accommodate the excessive fat and, at the same time, manage and/or compensate for the less-than-sufficient glucose (Boulangé, et al., 2013). Metabolite changes were thus investigated in large intestine by applying an OPLS-DA approach to compare animals fed a low fat control to those on a HF diet. As shown by OPLS-DA score plot (Figure 7A), the control clearly separated from the HF group. Based on the coefficient plot (Figure 7B), the levels of multiple metabolites in the HF group were elevated, including formate, fumarate, succinate, malate, PEP, acetate, AMP, GSSG. In contrast, decreased levels of oxalate, propionate, ATP, ADP, acetyl-CoA and most of the amino acids were also evident.

Acetyl-CoA is considered a metabolic intersection due to its connection with many metabolic pathways, such as glycolysis and the TCA cycle, fatty acid and amino acid metabolism, protein acetylation and DNA methylation (Carrer, et al., 2017). The flux of this intermediate in and out of mitochondria thus represents the metabolic state of a cell as “fed” or “starved” (Shi & Tu, 2015). Under conditions of sufficient glucose or a “fed” state, acetyl-CoA from glycolysis fluxes out of the mitochondria for fatty acid synthesis and storage (Shi & Tu, 2015). However,

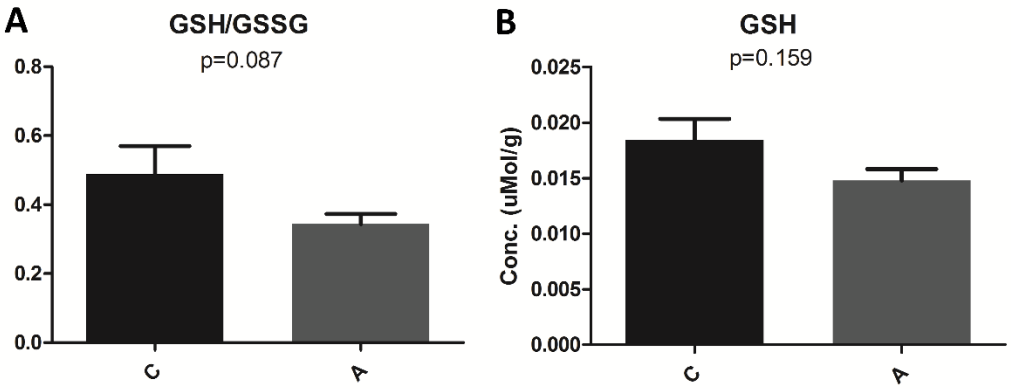

Figure 6 GSH/GSSG ratio and total glutathione in control and HF groups. Values are shown as the means ± SEM, n=11. Statistical differences were evaluated using non-parametric Kruskal-Wallis test.

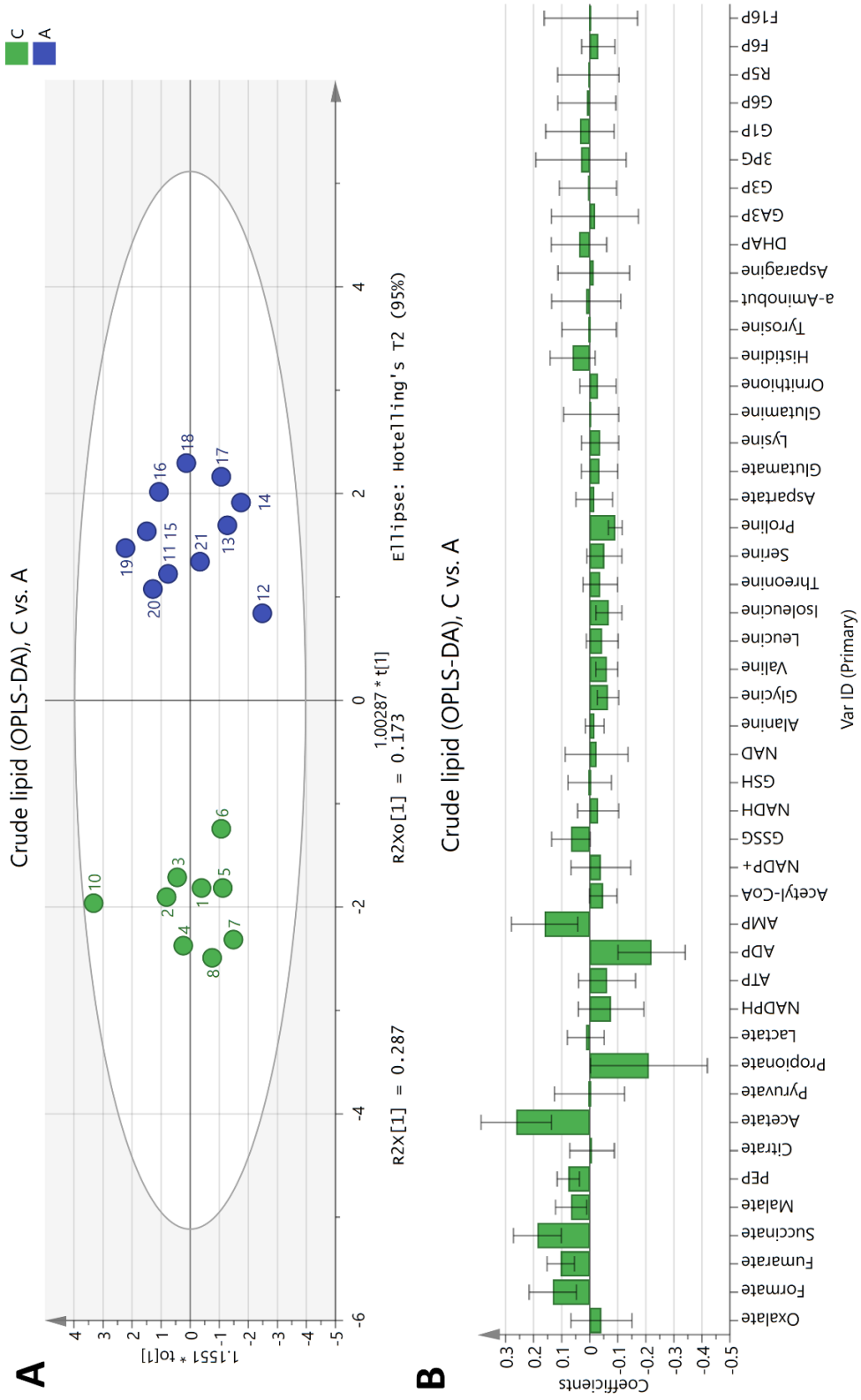

Figure 7 OPSD-DA score plot (upper) and coefficients (lower) for control and HF groups. Score plot R2X=0.46, R2Y=0.95, Q2=0.886. Positive bars (± SEM) of coefficient plot donate metabolites significantly increased when diet switch from control to HF.

under high fat and low carbohydrate conditions, a cell undergoes a pseudo starvation state by employing fatty acid β oxidation as a source for acetyl-CoA production. Most of the acetyl-CoA is maintained inside the mitochondria by inhibiting the activity of ATP citrate lyase (ACLY) (Carrer, et al., 2017), which catalyzes the conversion from acetyl-CoA to citrate. In the current experiment, the cellular net acetyl-CoA produced by the HF group was lower than that of the control group (p=0.112). Similarly, Carrer et al. (2017) reported a reduction of acetyl-CoA in a HF diet mice model. These results indicate that, as a source of acetyl-CoA, fatty acid is not as readily used and efficient as glucose, and the total generation of acetyl-CoA in a cell is slower when fatty acid is the major energy source (Fillmore, Mori, & Lopaschuk, 2014).

Due to the low acetyl-CoA and energy generation under HF diet, the cell is most likely restoring homeostasis by gluconeogenesis. Positioned at the very center of carbon metabolism, the TCA cycle functions as a metabolite hub, receiving carbon flow from different substrates and redirecting them to gluconeogenesis (Satapati, et al., 2012). As is shown in Figure 8, pyruvate reduction was not significant in HF group, but aspartate, which is convertible with OAA, decreased significantly (p=091). Combining the latter results with the significant increase in phosphoenolpyruvate (PEP) (p=0.002), and trending, but insignificant increase in glycerate-3-phosphate (3PG), glyceraldehyde-3-phosphate (GA3P) and glucose-1-phosphate (G1P), these changes indicates that HF group is undergoing mitochondria TCA anaplerosis from pyruvate to OAA followed by a cataplerosis from OAA to PEP (Sunny, Parks, Browning, & Burgess, 2011).

Pyruvate is not the only source of TCA anaplerosis as elevated amino acid anaplerosis has been reported on multiple studies conducted with HF diet animal models (An, et al., 2013) (Boulangé, et al., 2013) (Zha, et al., 2009). As is shown in Figure 9, amino acid catabolism was also higher in the HF group in a significantly large and wide scale. Ketogenic lysine and branch chain amino acid (BCAA) including leucine, isoleucine and valine significantly decreased combined with a decreasing, but insignificant, trend in glycogenic glutamate, proline, ornithine,

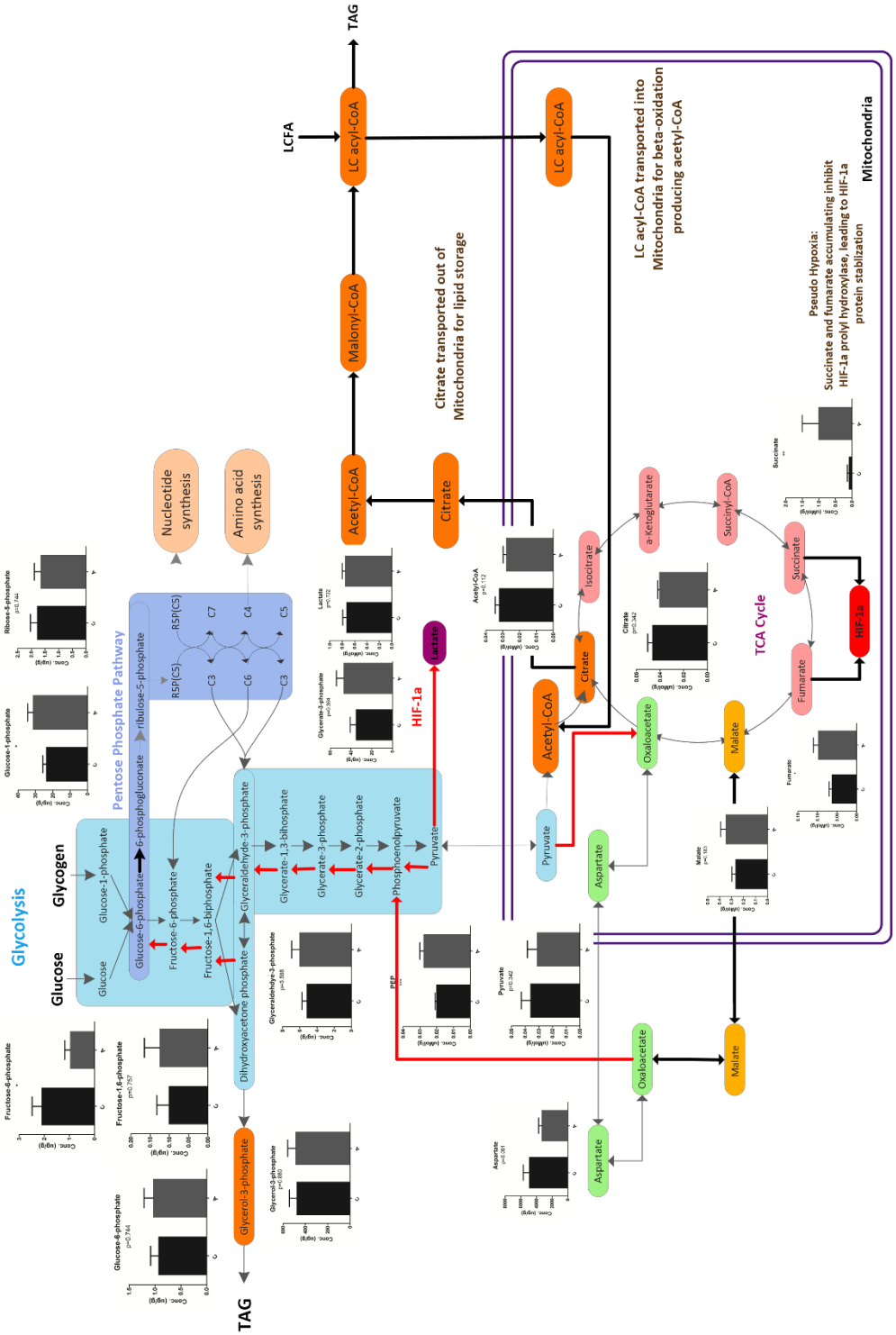

Figure 8 Central metabolism under HF influence. Values are shown in boxplot (upper whisker-upper quartile-median-lower quartile-lower whisker). Statistical differences were evaluated using non-parametric Kruskal-Wallis test.

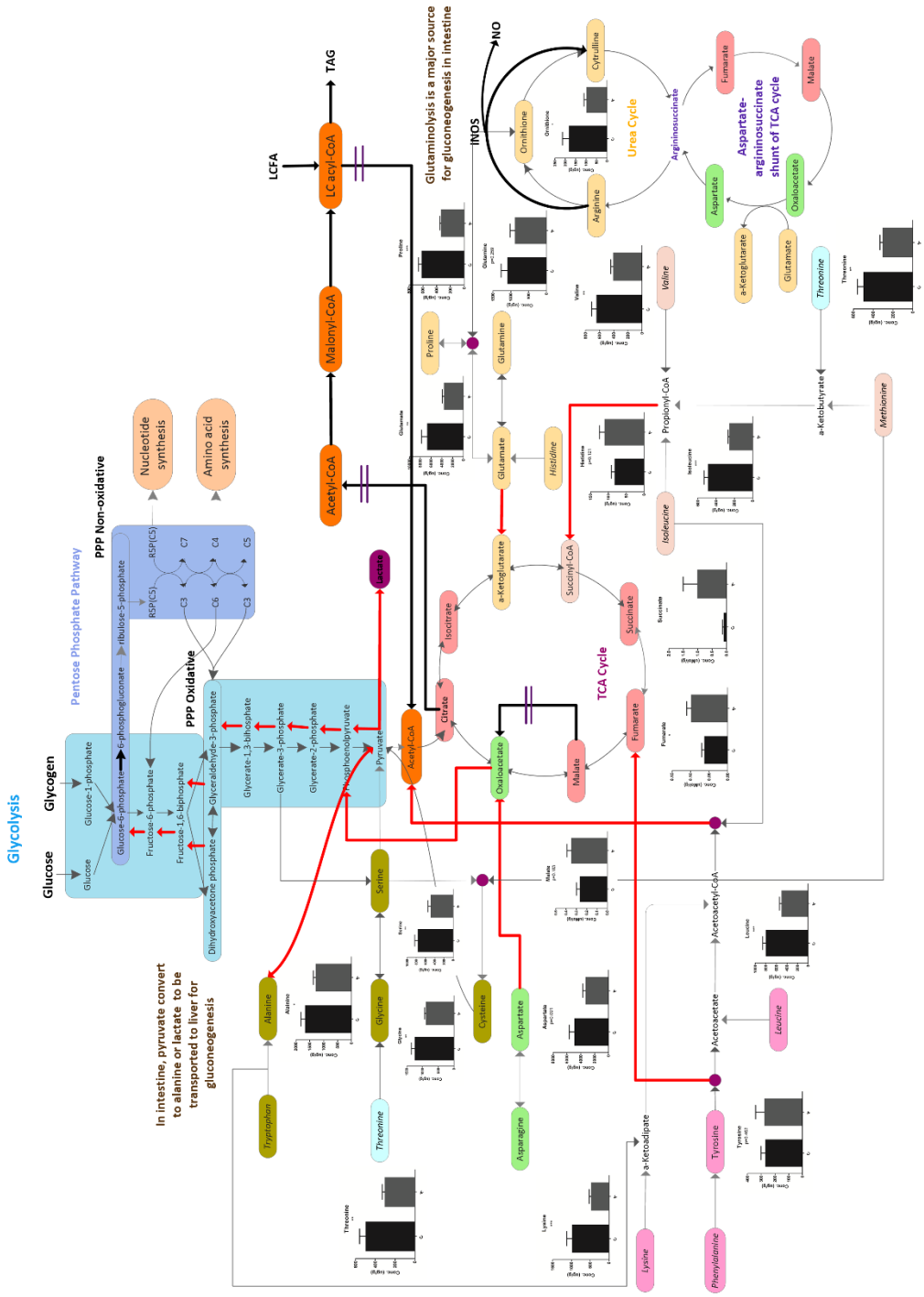

*Figure 9 Amino acid metabolism and gluconeogenesis under HF influence. Values are shown as the means ± SEM, n= 11. Statistical analysis ANOVA and Tukey's multiple comparison was conducted (***$p \leq 0.001$, **$p \leq 0.01$, *$p \leq 0.05$).*

threonine, glycine, serine and alanine. Other amino acids, including glutamine and aspartate also declined, albeit not significantly.

These results indicate that carbon flowed from amino acids and entered into the TCA cycle at different points, such as α-ketoglutarate, succinyl-CoA, fumarate, OAA and acetyl-CoA, thereby significant increasing TCA intermediates, especially succinate and fumarate (Figure 9). Satapati et al. (2012), An et al. (2013), and Boulangé et al. (2013) also reported elevated TCA metabolites in the presence of a HF diet. Satapati et al. (2012) proposed that the cells are in relatively oxidized redox state accompanied by a slower TCA cycle rate thereby causing other metabolic complications. For example, elevated fumarate and succinate have been shown to inhibit HIF-1α prolyl hydroxylase, resulting in hypoxia-inducible factor 1-alpha (HIF-1α) protein accumulation, which, in turn, causes a pseudo hypoxic cellular response (Koivunen, et al., 2007) (Selak, et al., 2005).

B. The impact of red grain sorghum crude lipid on central carbon metabolism in the presence of a HF diet

i. Effect of GS-CL supplements on HF stressors: energy and redox balance

Lee (2013) showed that lipids extracted from the whole kernel GS were able to modulate central carbon metabolism in both the liver and the large intestine of golden Syrian hamsters, but this study used fractioned oil and wax. In the current study, we show for the first time the impact that whole kernel GS-CL, that contains both the wax and oil fraction, has on cellular energy status in the presences of a HF diet. As is shown in Figure 10, energy charges obtained from three GS-CL supplemented groups all increased significantly, with the highest positive change occurring in the 3% GS-CL supplemented animals. This benefit, however, is not completely does-dependent, as the 5% group did not recover as well as 3% group. Improved energy charge could be attributed by two possible reasons, motivated mitochondria TCA cycle or activated AMP activated protein kinase (AMPK) complex (Wang, et al., 2015) (Kang, et al., 2015). Although experiment have yet

to be conducted to determine AMPK activity, a motivated TCA cycle was indeed observed in GS supplemented groups, which will be discussed in next session.

In terms of redox balance, the GS-CL was not able to reverse the low level of NAD+ and GSH caused by HF diet, GS-CL supplemented groups were not significantly different for either of these metabolites compared to the HF group (Figure 11A and Figure 12A). The metabolite, NADH remains nearly constant among all five groups (Figure 11B), yet there might be a slight upward trend in the NAD/NADH ratio to a ratio closer to the control occurred among the GS-CL supplemented groups in a dose dependent manner (Figure 11C).

The improvement in the GSH/GSSG ratio (Figure 12C) produced by 1% supplemented diet is certainly evident. Interestingly, it was achieved by breaking down GSSG without a concomitant increase in GSH (Figure 12B). (Reduction of 1mole GSSG to 2 moles GSH is catalyzed by glutathione reductase at the expense of NADPH, which was oxidized to NADP+ (Lushckak, 2012)). Incidentally, NADP+ in 1% group was higher compared to other groups (Figure 13B), which could be the reason for the significant reduction of GSSG. The whereabouts of the regenerated GSH from GSSG after reduction is illusive. However, GSH may have been used to elevate the activity of glutathione *S*-transferase (GST) enzymes and increased GSH detoxification capacity (Lushckak, 2012), but more studies are needed to test this hypothesis.

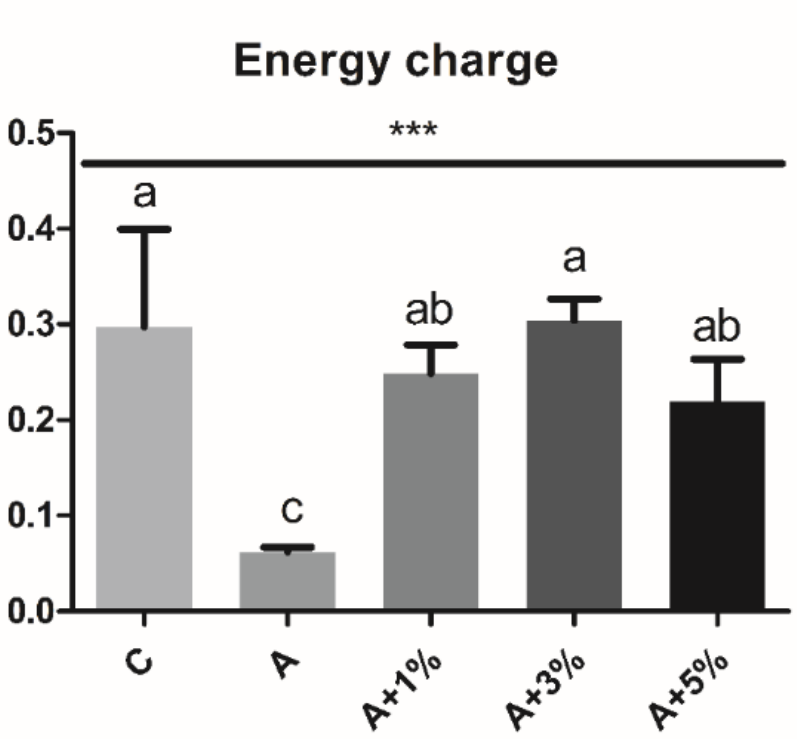

*Figure 10 Effect of GS-CL on cellular energy charge. Values are shown as the means ± SEM, n=11. Statistical analysis ANOVA and Tukey's multiple comparison was conducted (***p≤0.001).*

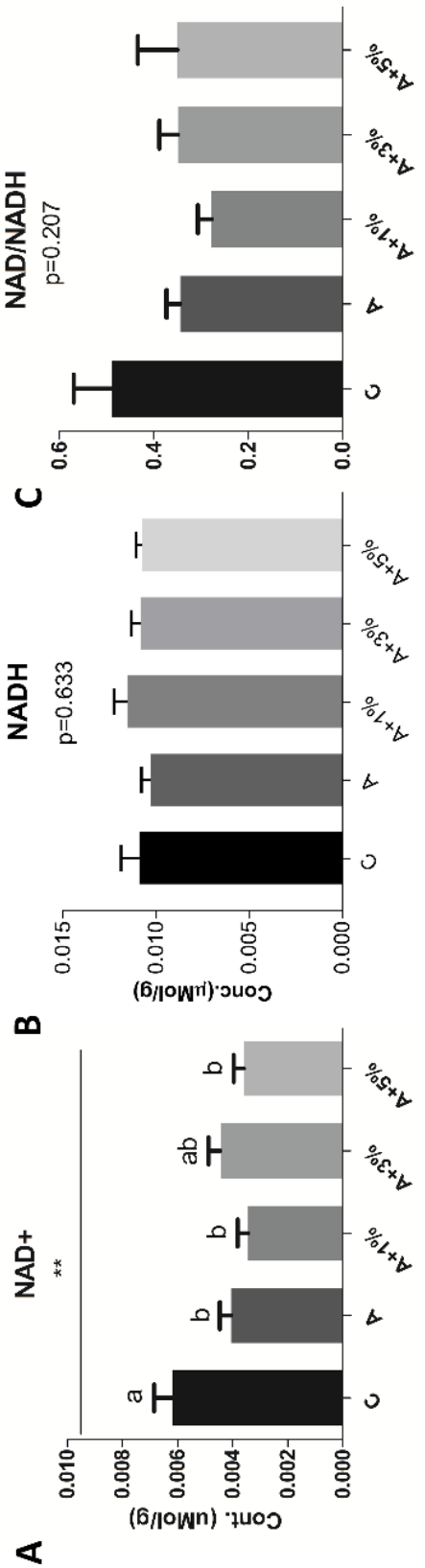

*Figure 11 Effect of GS-CL on NAD+, NADH and their ratio. Values are shown as the means ± SEM, n=11. Statistical analysis ANOVA and Tukey's multiple comparison was conducted (**p≤0.01).*

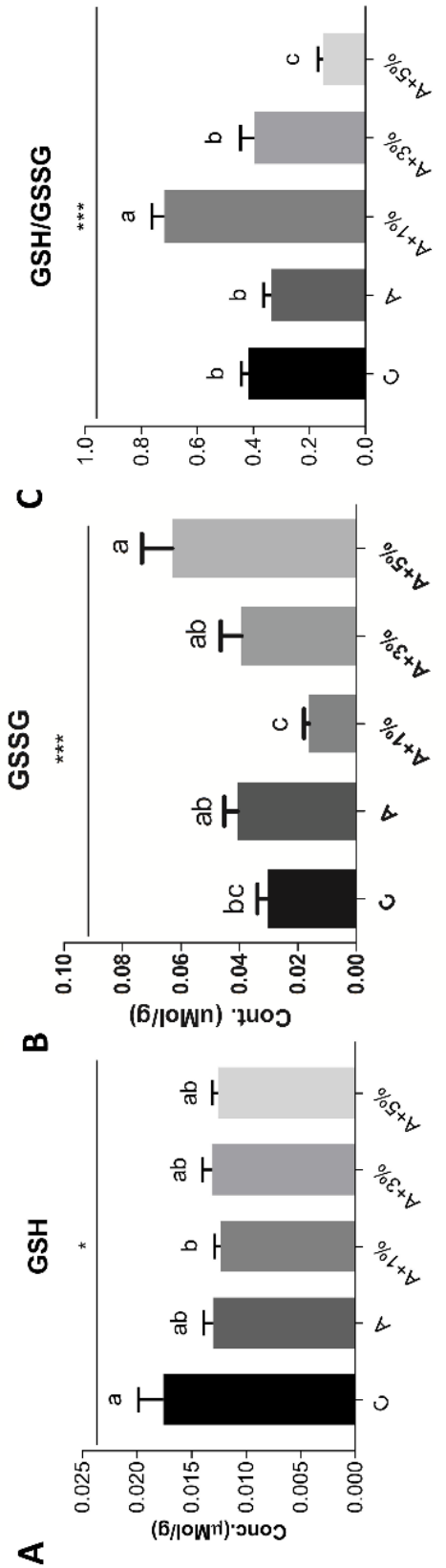

*Figure 12 Effect of GS-CL on GSH, GSSG and their ratio. Values are shown as the means ± SEM, n=11. Statistical analysis ANOVA and Tukey's multiple comparison was conducted (*p≤0.05, ***p≤0.001).*

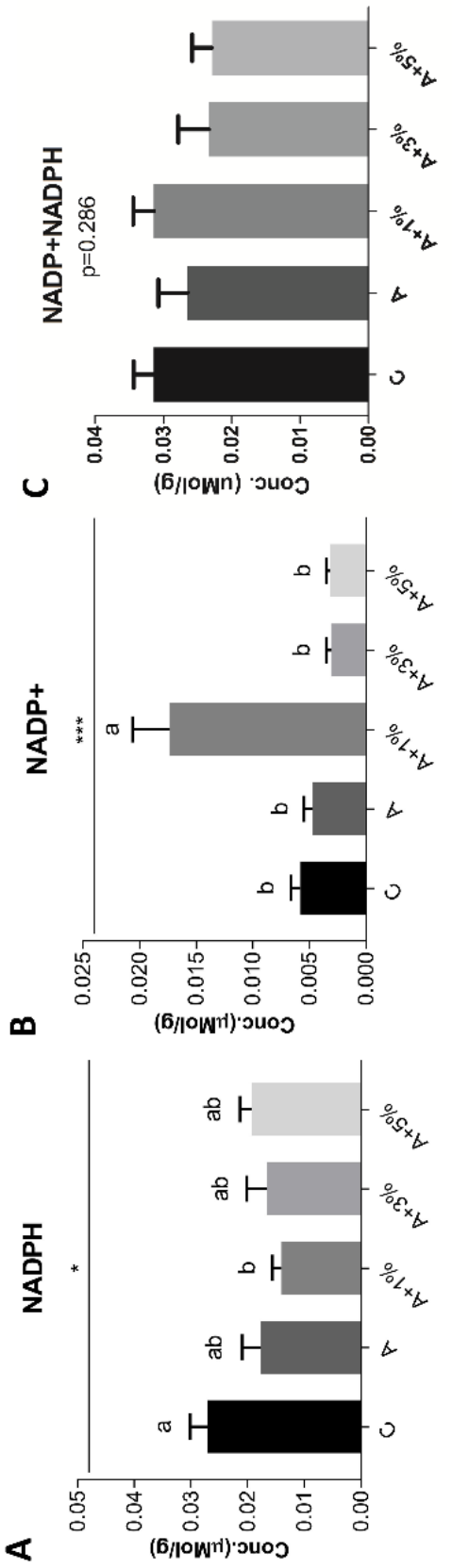

Figure 13 Effect of GS-CL on NADP+, NADPH and their ratio. Values are shown as the means ± SEM, n=11. Statistical analysis ANOVA and Tukey's multiple comparison was conducted ($p \leq 0.05$, ***$p \leq 0.001$).*

Other changes to metabolite redox couples may show additional insights into the cellular redox state (Figure 14). The malate-aspartate shuttle (MAS) and the glycerol-3-phosphate (G3P) shuttle are the primary and secondary pathways that are able to recycle glycolysis-generated cytosolic NADH back to NAD+. The shuttles are required because the mitochondrial inner membrane is impermeable to NADH (Easlon, Tsang, Skinner, Wang, & Lin, 2008). To circumvent this obstacle, malate and G3P transports the reducing equivalents into mitochondria (Easlon, Tsang, Skinner, Wang, & Lin, 2008), whereas the lactate/pyruvate couple recycles glycolytic NADH to NAD+ in the cytosol. Under normal aerobic condition, pyruvate enters the mitochondria for oxidative phosphorylation. In cases of hypoxia, mitochondria damages or elevated energy demand, however, pyruvate can also be reduced to lactate to facilitate NAD+ regeneration as a result of anaerobic respiration, or to compensate for the inability of MAS to keep pace with cytosolic NAD+ demand (Kane, 2014).

As is shown in Figure 14, the HF group presented with a considerably higher ratio of malate/aspartate, glycerol-3P/DHAP and lactate/pyruvate, indicating that the relative content of the electron carriers, malate, G3P and lactate, are elevated. As such, the HF group is in a relatively oxidized cellular state with respect to the control. In contrast, the 1% and 3% supplemented diets were able to lower each of these ratios in a does dependent manner. Interestingly, the 5% group exhibited elevated levels of all three ratios comparable to or even higher than the HF group. Further investigation of HIF-1α or mitochondrial electron transport chain complexes needs to be completed in order to determine the exact cause behind the latter results as they are the indicators for possible hypoxia and mitochondria damages, respectively.

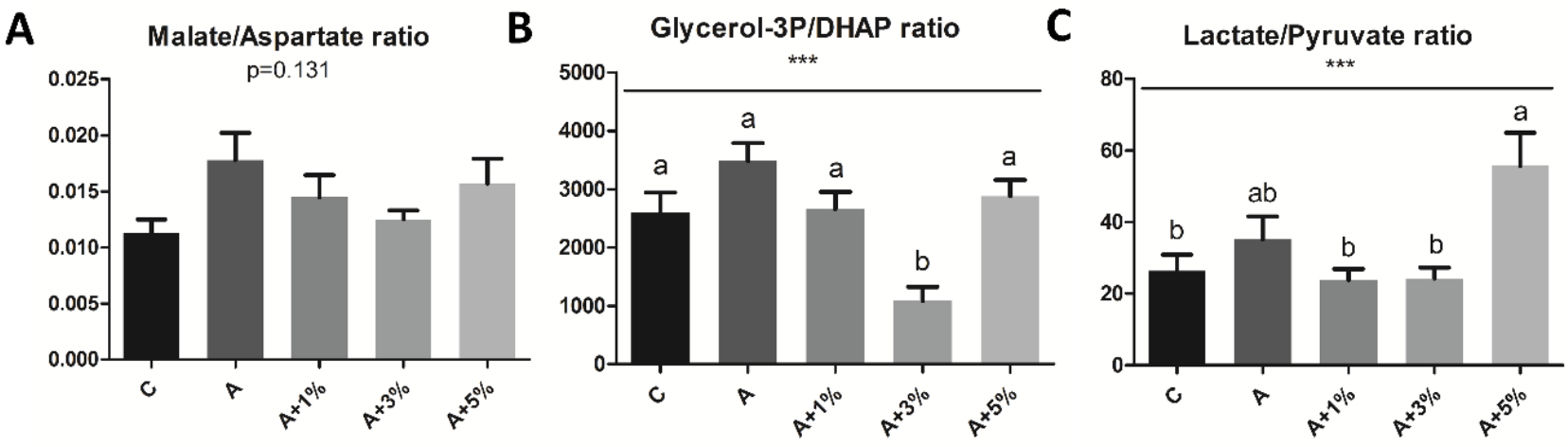

*Figure 14 Ratios of three metabolite redox couples among five diet groups. Values are shown as the means ± SEM, n=11. Statistical analysis ANOVA and Tukey's multiple comparison was conducted (***p≤0.001).*

ii. Effects of GS-CL supplements on HF stressors: key carbon metabolic pathways

An overview of global changes caused by diet and GS-CL supplements is illustrated by PLS-DA based on all the metabolite changes (Table 3) collected from all five groups in both 2D and 3D score plot (Figure 15). The control and HF group are clearly separated with the 1% group positioned in the middle, indicating a protective ability of GS-CL. The 3% group scatters across 1% and control group, representing the possibility of complete protection. Lastly, the 5% group is clustered further away from both the 1% and 3% groups but partially overlaps with HF group, further indicating that higher doses of GS-CL are less effective in modulating energy metabolism caused by a HF diet.

The three GS-CL supplement groups were analyzed via targeted metabolomics and compared with both HF and control groups using an OPLS-DA approach (shown in appendix), which in turn were summarized, as depicted in Figure 16. For the 1% GS-CL, the majority of elevated TCA metabolites caused by the HF diet were reduced back to the range of control group, i.e., malate (from 0.349 ± 0.041 µMol/g to 0.192 ± 0.027 µMol/g), fumarate (from 0.098 ± 0.011 µMol/g to 0.044 ± 0.007 µMol/g), and succinate (from 1.015 ± 0.488 µMol/g to 0.370 ± 0.128 µMol/g). It must be noted however, that citrate was not affected by the 1% GS-CL supplement. In addition, the 1% supplement was not able to stop the anaplerosis flow from pyruvate and amino acids caused by the HF diet. Pyruvate continued to decrease from 0.031 ± 0.006 µMol/g in HF group to 0.023 ± 0.002 µMol/g, while all the amino acids measured were even lower for 1% group compared to the HF animals. The anaplerosis flow for the 1% group is most likely slower than HF group as 3PG, GA3P and G1P are all lower, while PEP maintained the same level as HF group. In addition, the net content of acetyl-CoA (0.015 ± 0.000 µMol/g) is significantly lower than both control (0.032 ± 0.002 µMol/g) and HF groups (0.031 ± 0.003 µMol/g), implying that cells are still relying on fatty acid β oxidation as the main and slow energy source. Interestingly, glycerol-3-phosphate (G3P) decreased for the 1% group, indicating that the supplement may have the ability to restrict de novo triglyceride synthesis. These results concurs with the decreased

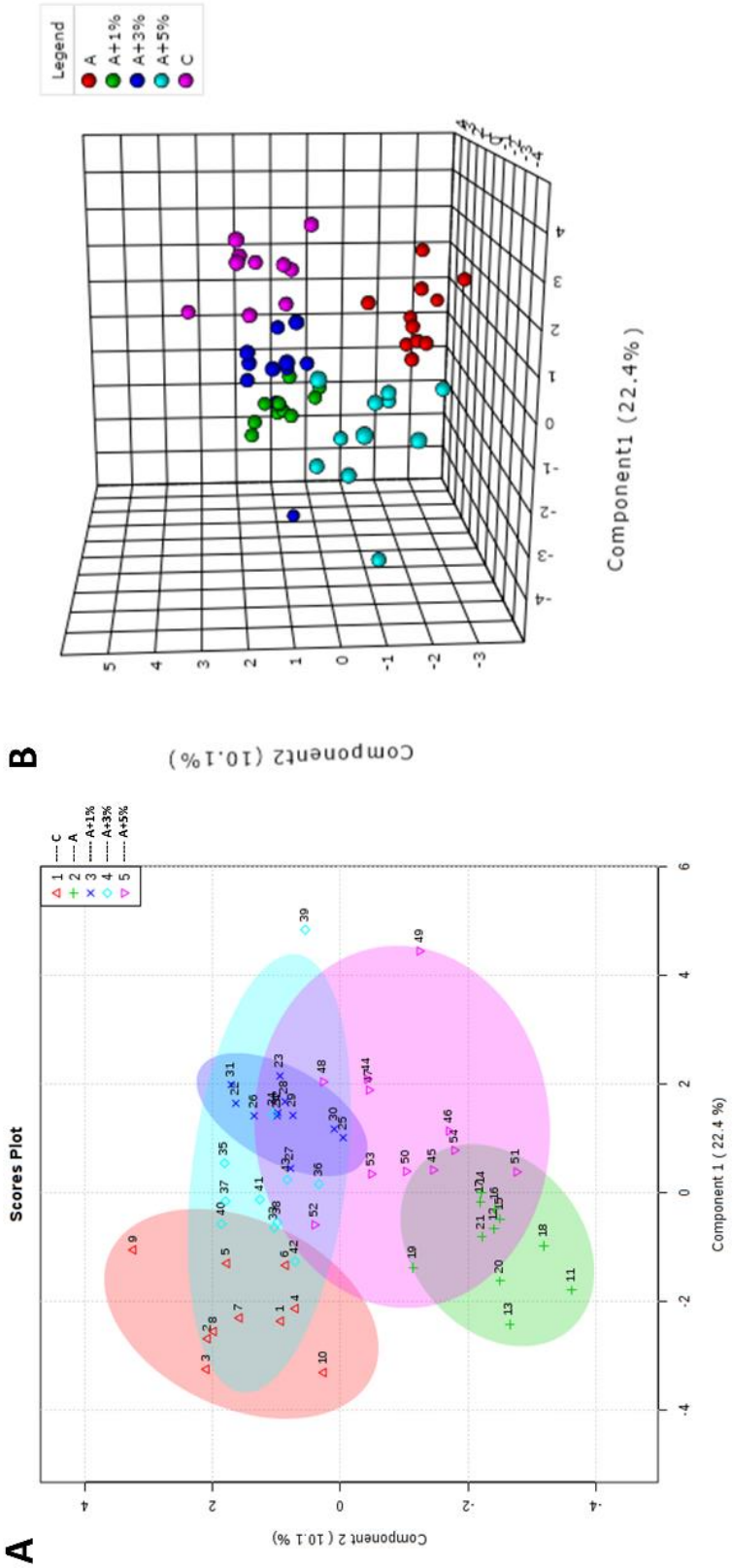

Figure 15 PLS-DA score plot for five treatment groups. (A) 2D score plot (two components, component 1 22.4%, component 2 10.1%). (B) 3D score plot (three components, component 1 22.4%, component 2 10.1%, component 3 8.5%). Each point represents one biological observation.

plasma triglycerides demonstrated by Althwab (2016). Specifically, the plasma triglyceride levels were reduced by 35% in hamsters fed with 1% red GS-CL supplemented HF diets compared with HF diet alone (Althwab, 2016).

By increasing the GS-CL supplement to 3%, the beneficial effects became more evident. Not only were the TCA metabolites malate (0.227 ± 0.025 µMol/g), fumarate (0.055 ± 0.008 µMol/g) and succinate (0.429 ± 0.214 µMol/g) as low as that of the 1% and control diets, but gluconeogenesis and anaplerosis flow slowed down prominently as well (Figure 16). Although pyruvate (0.024 ± 0.002 µMol/g) for the 3% group remained as low as 1% group, many of the amino acids were considerably higher than the HF group. Still, others, such as tyrosine, glutamate and glutamine, were restored completely similar to the low fat diet. Moreover, the glycolytic metabolites, 3PG, GA3P and G1P, decreased significantly to the level of the control group. Also G3P continued to decline in 3% group, suggesting a lasting restraining effect on triglyceride synthesis. Finally, acetyl-CoA (0.019 ± 0.001 µMol/g) started to recover in 3% group. Combined with slightly elevated citrate, these results indicate that the energy source begins to switch from fatty acid β oxidation back to glucose when a HF diet is consumed in the presence of 3% (w/w) GS lipid diet.

The 5% diet provides interesting and unexpected metabolic differences to both the 1% and 3% diets. Similar to the two lower GS-CL supplement doses, the 5% diet was able to sustain lower TCA metabolites, i.e., malate (0.208 ± 0.024 µMol/g), fumarate (0.060 ± 0.010 µMol/g) and succinate (0.124 ± 0.044 µMol/g). This diet also improved most of the amino acids levels relative to the 1% group. Some amino acids, such as alanine, serine and glycine, were restored completely, which was not achieved by the 3% group. Interestingly, however, the glycolytic metabolites 3PG and GA3P continued to decline with the noticeable exception of PEP (0.031 ± 0.003 µMol/g). The level of this intermediate was the highest among all five groups, suggesting accumulation of PEP. Moreover, lactate and G3P both spiked in 5% group, indicating that the cell is routing pyruvate toward lactate instead of the TCA cycle while directing the glycolytic sugar

phosphates toward triglyceride synthesis. In addition, acetyl-CoA (0.013 ± 0.001 µMol/g) reversed its upward trend exerted by the 3% diet, but rather was the lowest among the five groups. Based on this data, the 5% diet restricted the carbon flow from entering the TCA cycle, and channeled it towards lactate and triglycerides synthesis.

Overall, the 3% supplement diet was able to attenuate the damage on carbohydrate metabolism inflicted by HF diet with most of its metabolites approach values exhibited by the control group. The 3% diet was also able to stop the gluconeogenesis and anaplerosis from pyruvate and amino acids, motivated the TCA cycle and reduced the reliance of the cells on fatty acids. On the other hand, the 1% supplement diet was able to maintain a motivated TCA cycle, although the gluconeogenesis and anaplerosis was not halted. The 1% diet was not able to completely restore the deteriorating effect of a HF diet, but it did halt some of the changes in central metabolism. Lastly, the 5% GS-CL terminated anaplerosis from amino acids. However, carbon flow was restricted from entering the TCA cycle, which may due to the possible mitochondria damages caused by the increased fat burden of the 5% lipid supplement. Instead, this diet directed the carbon flow toward lactate and triglyceride synthesis.

III. Specific aim 2: GS-CL supplements modulate short chain fatty acid profile produced by gut microbiota

Short chain fatty acids (SCFA) are volatile fatty acids produced by gut microbiota in colon as fermentation products. These molecules are characterized by containing fewer than six carbons, existing in straight and branched-chain formation, among which, acetate (C_2), propionate (C_3) and butyrate (C_4) are the most abundant, representing 90% of the SCFA present in the colon (Ríos-Covián, et al., 2016). The biological effects of SCFA was reviewed in detailed by Ríos-Covián et al. (2016). More specifically, both butyrate and propionate have been reported to exert prominent effects in reducing inflammation and other diet-induced stressors, such as HF diets.

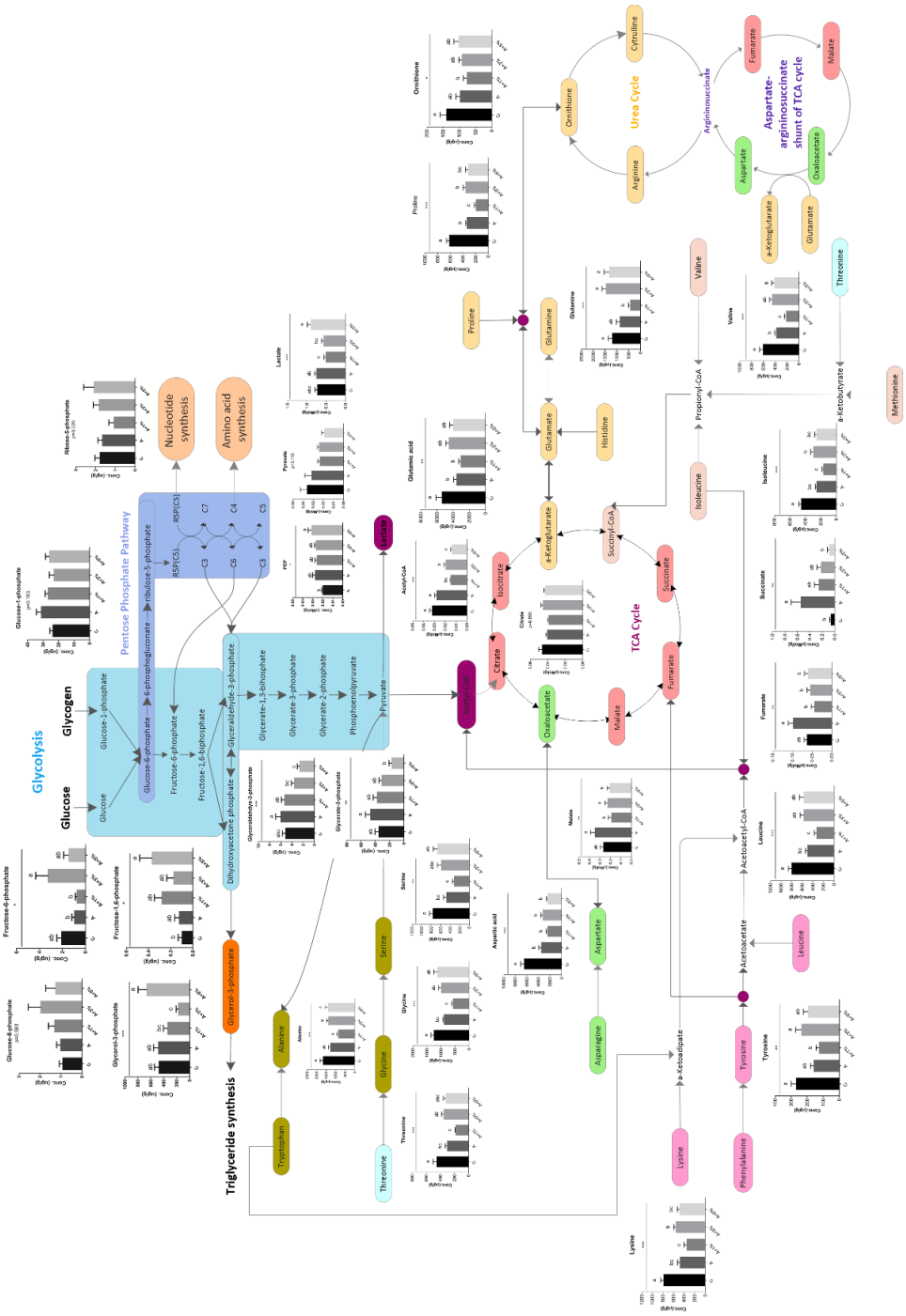

*Figure 16 The impact of GS-CL on central carbon metabolism. Values are shown as the means ± SEM, n=11. Statistical analysis ANOVA and Tukey's multiple comparison was conducted (***$p \leq 0.001$, **$p \leq 0.01$, *$p \leq 0.05$).*

For example, Jakobsdottir et al. (2013) demonstrated that a HF diet reduces the formation of SCFA on the whole and butyrate in particular in rats. In addition, the abundance of acetate-producing bacteria was increased in response to chronic HF diet consumption (Lecomte, et al., 2015).

The diet can also positively affect the gut microbiota composition and activity, and therefore the profile of synthesized SCFA (Brüssow & Parkinson, 2014). One such diet consists of high fiber and low fat diet, which has been characterized by higher levels of fecal SCFA (Cuervo, Salazar, Ruas-Madiedo, Gueimonde, & González, 2013). In the current experiment, the change in gut microbiota profile has yet to be determined, but the concentration of three most abundant SCFA was analyzed in five diet groups. The amount of acetate in HF and 5% supplement groups increased dramatically, over 10-fold higher compared to the control, 1% and 3% supplement groups (Figure 17A). Although butyrate was not detected in HF and 5% supplement groups, 1% and 3% supplement groups did produce a dose-dependent recovery in butyrate. Still, the latter two dosages were not able to completely remediate the effects caused by the HF diet as butyrate levels were higher in the control group (Figure 17B). For propionate, all HF groups with or without GS-CL supplement were lower compared to the control group. It is further noticeable that the 5% group presented with even lower levels of propionate than the HF group (Figure 17C).

Based on the data, the 3% GS-CL supplement demonstrated the optimal protection of the SCFA profile against HF-induced stress followed by the 1% supplement. The 5% supplement group did not show any improvement when compared to HF group. This trend is also exemplified in the acetate: propionate ratio (Figure 17D). As acetate is a substrate involved in cholesterol synthesis via acetyl-CoA, it is generally preferable to have a low acetate: propionate ratio (Jakobsdottir, Xu, Molin, Ahrné, & Nyman, 2013). The 1% and 3% supplement groups showed a low acetate: propionate ratio comparable to the control group whereas 5% supplement group is comparable to the HF group.

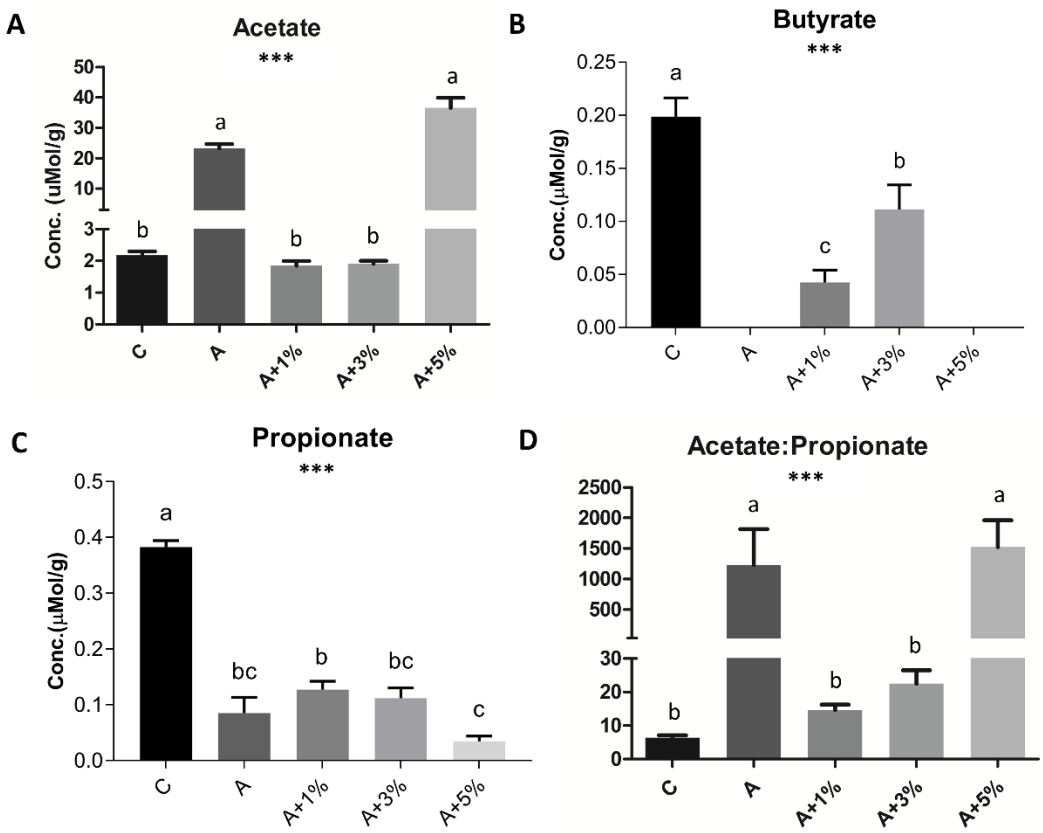

*Figure 17 Effect of GS-CL on short chain fatty acid profile. Values are shown as the means ± SEM, n=11. Statistical analysis ANOVA and Tukey's multiple comparison was conducted (***p≤0.001).*

IV. Specific aim 3: Characterization of red grain sorghum *(sorghum bicolor)* whole kernel crude lipid

A. Characterization of red GS-CL

Determination of the whole kernel red GS-CL showed yields of 0.2-0.4% on a dry weight basis, which is similar to that reported by Hwang et al. (2004). Christiansen (2008) produced a higher yield (0.6%), but a solvent to solid ratio of 3:1 was employed compared to the 1:1 ratio used in this study, which may have caused the yield variability. For example, total lipid yield is influenced by the method of its extraction (Christiansen K. , Weller, Schlegel, & Dweikat, 2008). However, for GS, the difference of extraction method is only significant for the ground GS and GS-DDGS, indicating that the lipid yield of whole kernel GS is not affected by the method of extraction (Leguizamón, Weller, Schlegel, & Carr, 2009). In addition, Leguizamón (2009) showed that the form of GS is substantially affects lipid yields. Lipid yields obtained of GS-DDGS was higher lipid compared to either ground or whole kernel GS as the non-starch compounds are concentrated after fermentation. Although ground GS does not produce as much lipid as GS-DDGS, ground GS yields higher amount of lipid compared to the whole kernel GS due to increased surface area. Indeed, Hwang et al. (2004) reported a lipid yield of 0.5-0.6% from GS-DDG, much higher than the yield of 0.2-0.3% from GS whole kernel.

Further characterization of the red whole kernel lipid, as depicted by TLC (Figure 18),showed the presence of monoacylglycerols, diacylglycerols, triacylglycerols, fatty acids, fatty aldehydes, fatty alcohols (policosanols), free sterols (phytosterols), wax/steryl easters and hydrocarbons. These results concur with the TLC analysis reported by Carr et al. (2005).

Among TLC shown lipid categories, phytosterols and policosanols are of particular interest due to their many health benefiting effects, including cholesterol management, improving blood lipid profile and anti-cancer (Carr, Ash, & Brown, 2010) (Awad & Fink, 2000) (Gouni-Berthold & Berthold, 2002). For the whole kernel red GS-CL, phytosterols were present at 4.93 ±

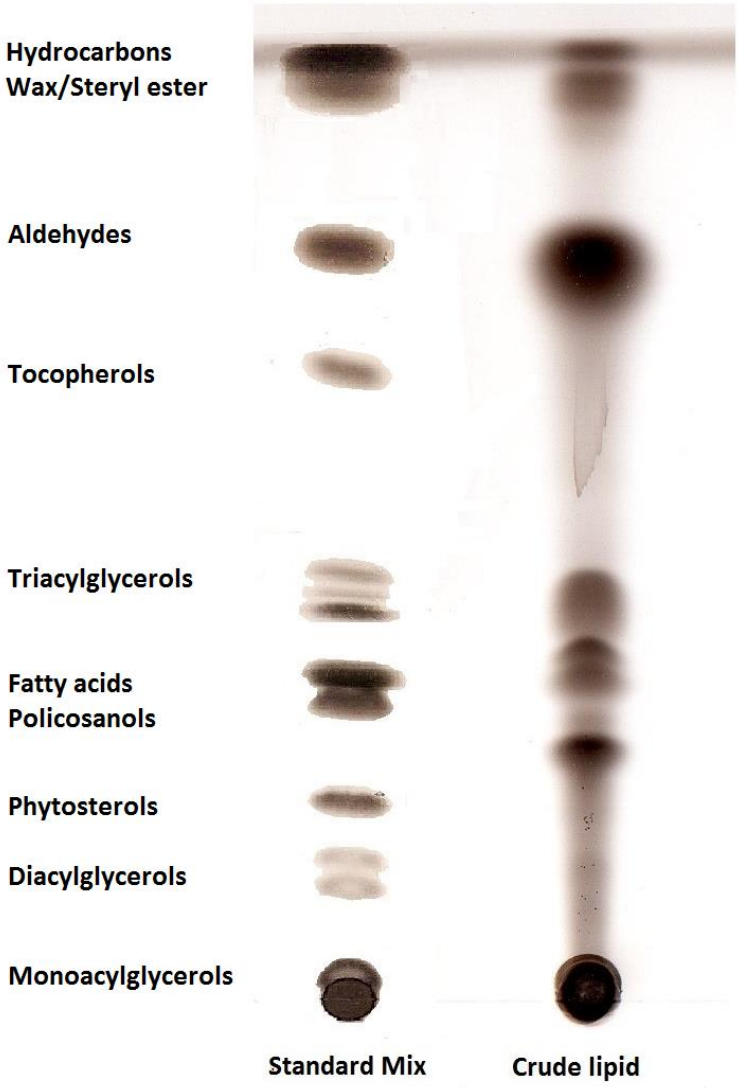

Figure 18 The simple lipid profile of GS-CL analyzed by thin layer chromatography (TLC). Lipid was spotted on silica plate and developed with hexane: diethyl ether: acetic acid (85:15:2, by volume). The plate was visualized by submerged briefly in 10% cupric sulfate, 8% phosphoric acid solution, air-drying in a chemical fume hood before charring in an oven at 165°C for 10min.

0.05 mg/g lipid total phytosterols with β-sitosterol being the most abundant (58.7%), followed by campesterol (24.3%) and stigmasterol (16.9%) (Table 3). These results were slightly higher than the 3.48 mg/g lipid and 2.98 mg/g lipid reported by Carr et al. (2005) and Leguizamón et al. (2009), respectively. In addition, the prevalence of these three phytosterols is supported by a study performed by Leguizamón et al. (2009). However, Christiansen (2007) reported that stigmasterol was the most abundant phytosterol in whole kernel lipid extracts of nine different parent lines of GS, which was probably due to the co-elution between stigmasterol and triacontanol (C_{30}). In addition, extraction time and method (Winkler, Rennick, Eller, & Vaughn, 2007), and hydrolysis and saponification during sample preparation (Piironen, Toivo, & Lampi, 2002) can also affect the yield of phytosterols.

The level of total policosanols in red GS-CL was 15.61 ± 0.6 mg/g with octacosanol (C_{28}) (50.9%) and hexacosanol (C_{26}) (40.4%) being the major components. It must be emphasized that the extracts obrained from the red whole kernel GS contained higher policosanols compared to 8mg/g lipid measured by Carr et al. (2005), but lower compared to 18.82 mg/g lipid measured by Leguizamón et al. (2009). Although Leguizamón et al. (2009) also reported high levels of octacosanol (51.5%) and hexacosanol (24.5%), they detectedonly 21.2% of triacontanol (C_{30}) and very little of dotriacontanol (2.8%). Similar to that of the total lipid, the yield of policosanols are much higher from GS-DDG than that of GS whole kernel (Hwang, Weller, Cuppett, & Hanna, 2004). Policosanols, mostly long-chain fatty acids, tend to remain intact during the ethanol fermentation process, hence are likely concentrated in DDG form. Interestingly, Hwang et al. (2004) also reported fairly high percentage of triacontanol (C_{30}, 40-43%) yield.

Similar to other cereal groups, triacylglycerols is one of the most abundant lipid classes present in whole kernel GS lipid extract (Lee, et al., 2011). Fatty acid analysis showed that linoleic acid, oleic acid and palmitic acid are the predominant fatty acid classes in whole kernel red GS-CL (Figure 19), together comprising up to 88.8% fatty acids. Carr et al. (2005) reported

Table 3 Other composition of GS-CL.

Compound	Composition	Content
Phytosterols[1]	Total amount (mg/g lipid)	4.93 ± 0.05mg
	β-Sitosterol	58.7%
	Stigmasterol	16.9%
	Campesterol	24.3%
Policosanols[1]	Total amount (mg/g lipid)	15.61 ± 0.6mg
	Hexacosanol (C_{28})	40.4%
	Octacosanol (C_{26})	50.9%
	Dotriacontanol (C_{32})	8.7%
Vitamin E[2]	As mg α-Tocopherol per g lipid	0.068 ± 0.007mg
Carotenoids[3]	Total amount (μg/g lipid)	0.77 ± 0.04μg
Tannins[4]	As mg catechin per g lipid	0.278 ± 0.008mg

[1] Phytosterols and policosanols were determined by GC-FID as described by Leguizamón et al. (2009);
[2] α-Tocopherols was analyzed by a spectrophotometer as described by Wong et al. (1988);
[3] Carotenoids were determined by a spectrophotometer as described by Lichtenthaler & Buschmann (2001);
[4] Tannins were determined by a spectrophotometer as described by Bhat et al. (2007).

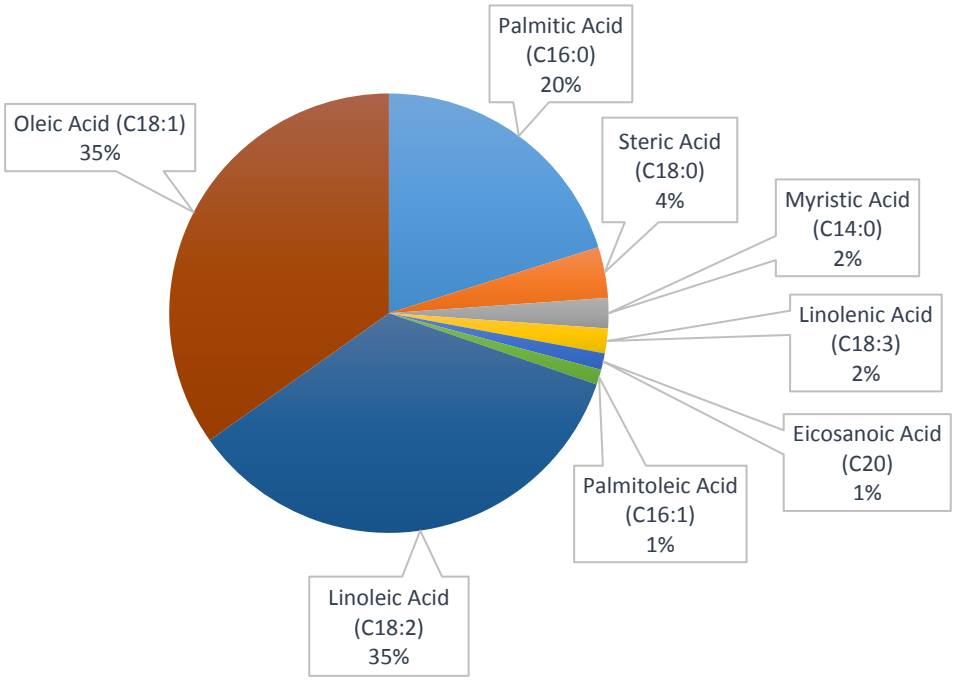

Figure 19 The fatty acid profile of GS-CL. Fatty acids were analyzed by GC-FID after methylation as described by Metcalfe et al. (1966). Percentage results from the cited compositional analyses are based on relative amounts.

similar fatty acid composition of 17% palmitic acid, 35% oleic acid and 41% linoleic acid. Christiansen (2006) noted that the lipid extract from ground GS contains more triacylglycerols and diacylglycerols while whole kernel GS lipid extract contains more policosanols and phytosterols. These results indicates that the health benefiting policosanols and phytosterols are located mainly in the coating lipid covering the kernel surface.

In addition, micronutrients, including carotenoids, tocopherols and tannins were also determined. The whole kernel GS-CL contains 0.068 mg/g lipid tocopherols, higher than the two GS parent lines studied by Christiansen (2007) (21.9 mg and 57.7 mg per 100 g lipid). Also, the red GS-CL contains 0.278 mg/g lipid tannins. Most of the GS cultivated in the US are tannin-free due to their impact on the digestibility of many nutrients, but the selected red GS in this study contains high tannin for the purpose of studying their part in the health benefiting effect of GS lipid extract. Lastly, the whole kernel GS-CL contains 0.77 μg/g lipid carotenoids.

B. Possible links between red GS-CL composition and its effects on central carbon metabolism

The health promoting properties of bioactive compounds are connected to its composition. The effects of red GS-CL on central carbon and energy metabolism discussed in previous chapter reflect the combined effects of each component and the additive, synergistic or antagonizing interactions among them. The major bioactive components in GS-CL, such as phytosterols and policosanols, exert their own effect on central carbon metabolism, although metabolic studies of these individual components remains limited as research on phytosterols and policosanols are mainly focusing on its regulation on cholesterol and lipid metabolism (Carr, Ash, & Brown, 2010) (Gouni-Berthold & Berthold, 2002). Nevertheless, Lee et al. (2015) showed that barley sprout extracts (BSE) containing 5.74 mg/g policosanols affected hepatic glucose metabolism in HF diet fed C57BL/6J mice model. The BSE supplement reduced fasting glucose level by repressing hepatic gluconeogenesis genes, including fructose-1,6-biphosphatase and pyruvate carboxylase (Lee, et al., 2015). Researchers further concluded that the activation of AMPK was responsible for this repression. In addition, aloe vera phytosterol extracts suppressed hyperglycemia and lowered both basal and fasting blood glucose levels in obese diabetic Zucker rats (Misawa, et al., 2008). The phytosterol extracts repressed gluconeogenesis by lowering the expressions of glucose-6-phosphatase and phosphoenolpyruvate carboxylase (PEPCK) and promoted glycolysis by increasing the mRNA level of glycolysis enzyme glucokinase (GK) (Misawa, et al., 2012). This beneficial effects of phytosterols in glucose metabolism can also be traced back to its role in activating AMPK (Hwang, et al., 2008).

In the current study, gluconeogenesis caused by HF diet was partially mitigated by GS-CL, especially in 3% GS-CL supplement group. Although the gene expression of pyruvate carboxylase and PEPCK, which catalyze the gluconeogenic conversion of pyruvate to OAA and OAA to PEP, respectively, have yet to be measured in this study, the suppression on

gluconeogenesis by 1% and 3% GS-CL was evident by an increase in pyruvate and an decrease in PEP. In addition, decreases in GA3P and 3PG presented by the supplemented groups indicated that the rate of glycolysis was partially restored by GS-CL. Kim and Park (2012) have showed that sorghum ethanol extract increases the phosphorylation of AMPK in streptozotocin-induced diabetic rats. It is therefore possible that the results in the current experiment is connected to the policosanols and phytosterols in GS-CL, which regulate the key gluconeogenesis and glycolysis enzymes by activating of AMPK.

5. Conclusion and future studies

Grain sorghum is a widely cultivated yet critically underutilized crop in the US. The crude lipid located on the surface of the whole kernal is of particular interest due to its unique phytochemical profile and beneficial regulatory effects on plasma and liver cholesterol and gut microbiota. In order to explore its impact on cellular central carbon and energy metabolism, GS-CL was supplemented to a HF diet in 1, 3 and 5% dosage and fed to a hamster model for 4 weeks period in comparison to a normal control diet and a HF diet.

The HF diet alone caused severe impairment in the ability of a cell to generate energy and disrupted cellular redox balance in hamster large intestine. The excessive fat supply forced the cells to reprogram its central carbon metabolism to use fat instead of glucose as the major energy source in order to accommodate excessive fat and compensate for the insufficient glucose supply. Many of amino acids as well as pyruvate are depleted greatly substantially when a system is in a gluconeogenesis state. These compounds thus enter the TCA cycle from different point, resulting in accumulated TCA cycle intermediates and elevated glycolytic intermediates.

The GS-CL supplements was able to restore the ability of the cells to generate energy as energy charges obtained from three GS-CL supplemented groups all increased significantly. However, they were not able to completely restore the redox balance disrupted by the HF feeding as GSH and NAD+ levels were as low as HF group. Yet slight upward trend in NAD+/NADH and GSH/GSSG ratios occurred possibly showing a long term protective effect based on feeding time or dosage levels. Multivariant analysis showed that the 3% supplement diet was the optimal diet in terms of protecting against damages to central carbon metabolism inflicted by HF diet by activating the TCA cycle and glycolysis as well as suppressing gluconeogenesis similar to that exerted by a low fat diet. The 1% supplement diet was not able to suppress anaplerosis from amino acids but gluconeogenesis was halted and the TCA metabolic rate increased. The 5% supplement diet was able to suppress anaplerosis from amino acids and motivate the TCA cycle,

but resulted in increasing gluconeogenesis, most likely due to contributing to the overall fat content. As a result, carbon flow towards lactate and triglyceride synthesis increased. For SCFA production in response to GS-CL dosage levels, the 5% supplemented diet performed similar to the HF diet while the 1% and 3% supplemented diets produced SCFA levels similar levels to the control diet.

Results obtained from the current study should be used as a stepping stone, upon which new theories and hypothesis can be built. In this study, cellular energy generation was severely impaired by the HF diet, resulting in a considerably low energy charge in that group. Cellular redox balance was also disrupted by the HF diet presented by a significantly lower NAD/NADH ratio. It is possible that the excessive fat from the HF diet accumulated in mitochondria for β oxidation, which damages the electron transport chain, thereby reduces the ability of the cells to generate energy and recycle NADH. Analysis regarding the activity of electron transport chain needs to be performed. In addition, elevated TCA cycle intermediates fumarate and succinate in the HF group could lead to HIF-1α protein accumulation. As a transcription factor, HIF-1α binds to nuclear, signaling a pseudo hypoxic cellular response (Koivunen, et al., 2007) (Selak, et al., 2005) and possibly initiate inflammation. Quantitative analysis of HIF-1α protein and pro-inflammatory cytokine NF-κB and TNF-α are needed in order to understand the mechanism. Moreover, the impact of GS-CL on SCFA profile is not fully understood until microbiome study is performed on the fecal samples collected from all five groups. The GS-CL probably regulated a single or multiple species in the gut microbiome resulting in the changes shown in SCFA profile.

The metabolic impact of GS-CL can be traced back to its composition. The red GS-CL used in this experiment contained high levels of phytosterols and policosanols, both of which have shown promoting effects on glycolysis and suppressing effects on gluconeogenesis by activating the AMPK in the cell (Lee, et al., 2015) (Misawa, et al., 2012). Moreover, it is possible that the GS-CL improved cellular energy state through activating AMPK because improved

energy state can be attributed to AMPK activation (Wang, et al., 2015) (Kang, et al., 2015). The phosphorylation and activity of AMPK need to be analyzed in all five groups, which will assist understanding how the GS-CL protect the cells against HF induced damages on central carbon metabolism, the connection between its composition and function.

Lee (2013) fractioned white GS-CL into oil and wax, and determined that the phytosterols and policosanols are present in the oil and wax fraction, respectively. Both fractions were then administered to each HF diet hamster model. Metabolic analysis of the intestinal tissue show different impacts exerted by the two fraction groups (Lee, 2013). Therefore, it is recommended that red GS-CL can also be separated into oil and wax fractions to understand how each may reprogram cellular central metabolism differently compared to either the red GS-CL or white GS fractions. The possible synergistic, antagonizing or simple additive interactions between the two fractions may well further our understanding towards this novel healthy promoting extract.

References

Ademiluyi, A. O., Oboh, G., Agbebi, O. J., & Oyeleye, S. I. (2014). Dietary inclusion of sorghum (Sorghum bicolour) straw dye protectsagainst cisplatin-induced nephrotoxicity and oxidative stress in rats. *Pharmaceutical Biology, 52*(7), 829-34.

Ajiboye, T. O., Komolafe, Y. O., Oloyede, H. O., Yakubu, M. T., Adeoye, M. D., Abdulsalami, I. O., . . . Akanji, M. A. (2013). Diethylnitrosamine-induced redox imbalance in rat microsomes: protective role of polyphenolic-rich extract from Sorghum bicolor grains. *Journal of Basic and Clinical Physiology and Pharmacology, 24*(1), 41-9.

Ajiboye, T., Iliasu, G., Adeleye, A., Ojewuyi, O., Kolawole, F., Bello, S., & Mohammed, A. (2016). A fermented sorghum/millet-based beverage, Obiolor, extenuates high-fat diet-induced dyslipidaemia and redox imbalance in the livers of rats. *Journal of the science of food and agriculture, 96*(3), 791-7.

Althwab, S. (2016). *Ability of crude lipid, wax, and oil fractions extracted from red grain sorghum whole kernel to prevent high cholesterol caused by high-fat diets in a hamster model*. Lincoln: University of Nebraka-Lincoln.

Althwab, S., Carr, T. P., Weller, C. L., Dweikat, I. M., & Schlegel, V. (2015). Advances in grain sorghum and its co-products as a human health promoting dietary system. *Food research international, 77*(3), 349-59.

An, Y., Xu, W., Li, H., Lei, H., Zhang, L., Hao, F., . . . Tang, H. (2013). High-fat diet induces dynamic metabolic alterations in multiple biological matrices of rats. *Journal of proteome research, 12*(8), 3755-68.

Atkinson, D., & Walton, G. (1967). Adenosine triphosphate conservation in metabolic regulation. Rat liver citrate cleavage enzyme. *The journal of Biological chemistry, 242*(13), 3239-41.

Awad, A. B., & Fink, C. S. (2000). Phytosterols as anticancer dietary components: evidence and mechanism of action. *The Journal of nutrition, 130*(9), 2127-30.

Awika, J. M., & Rooney, L. W. (2004). Sorghum phytochemicals and their potential impact on human health. *Phytochemistry, 65*(9), 1199-221.

Bastie, C., Gaffney-Stomberg, E., Lee, T., Dhima, E., Pessin, J., & Augenlicht, L. (2012). Dietary cholecalciferol and calcium levels in a Western-style defined rodent diet alter energy metabolism and inflammatory responses in mice. *142*(5), 859-65.

Bekkering, S., Quintin, J., Joosten, L. A., van der Meer, J. W., Netea, M. G., & Riksen, N. P. (2014). Oxidized low-density lipoprotein induces long-term proinflammatory cytokine production and foam cell formation via epigenetic reprogramming of monocytes. *Arteriosclerosis, thrombosis, and vascular biology, 34*(8), 1731-8.

Benson, K. F., Beaman, J. L., Ou, B., Okubena, A., Okubena, O., & Jensen, G. S. (2013). West African Sorghum bicolor Leaf Sheaths Have Anti-Inflammatory and Immune-Modulating Properties In Vitro. *Journal of Medicinal Food, 16*(3), 230-8.

Beyaz, S., Mana, M., Roper, J., Kedrin, D., Saadatpour, A., Hong, S., . . . Yilmaz, O. (2016). High-fat diet enhances stemness and tumorigenicity of intestinal progenitors. *Nature, 531*(7592), 53-8.

Bhat, R., Sridhar, K., & Tomita-Yokotani, K. (2007). Effect of ionizing radiation on antinutritional features of velvet bean seeds (Mucuna pruriens). *Food chemistry, 103*(3), 860-6.

Boulangé, C., Claus, S., Chou, C., Collino, S., Montoliu, I., Kochhar, S., . . . Martin, F. (2013). Early metabolic adaptation in C57BL/6 mice resistant to high fat diet induced weight gain involves an activation of mitochondrial oxidative pathways. *Journal of proteome research, 12*(4), 1956-68.

Bralley, E., Greenspan, P., Hargrove, J. L., & Hartle, D. K. (2008). Inhibition of Hyaluronidase Activity by Select Sorghum Brans. *Journal of Medicinal Food, 11*(2), 307-12.

Brüssow, H., & Parkinson, S. (2014). You are what you eat. *Nature biotechnology, 32*(3), 243-5.

Burdette, A., Garner, P. L., Mayer, E. P., Hargrove, J. L., Hartle, D. K., & Greenspan, P. (2010). Anti-Inflammatory Activity of Select Sorghum (Sorghum bicolor) Brans. *Journal of medicinal food, 13*(4), 879-87.

Burdette, A., Hargrove, J. L., Hartle, D. K., & Greenspan, P. (2007). Development of sorghum bran as an anti-inflammatory nutraceutical. *The FASEB Journal, 21*, 550.28.

Carbonero, F., Benefiel, A., Alizadeh-Ghamsari, A., & Gaskins, H. (2012). Microbial pathways in colonic sulfur metabolism and links with health and disease. *Frontiers in physiology, 28*(3), 448.

Carr, T. P., Ash, M. M., & Brown, A. W. (2010). Cholesterol-lowering phytosterols: factors affecting their use and efficacy. *Nutrition and dietary supplements, 2*, 59-72.

Carr, T. P., Weller, C. L., Schlegel, V. L., Cuppett, S. L., Guderian, D. M., & Johnson, K. R. (2005). Grain Sorghum Lipid Extract Reduces Cholesterol Absorption and Plasma Non-HDL Cholesterol Concentration in Hamsters. *The journal of nutrition, 135*(9), 2236-40.

Carrer, A., & Wellen, K. (2015). Metabolism and epigenetics: a link cancer cells exploit. *Current opinion in biotechnology, 34*, 23-9.

Carrer, A., Parris, J., Trefely, S., Henry, R., Montgomery, D., Torres, A., . . . Wellen, K. (2017). Impact of a High-fat Diet on Tissue Acyl-CoA and Histone Acetylation Levels. *The Journal of biological chemistry, 292*(8), 3312-22.

Carter, P. R., Hicks, D. R., Oplinger, E. S., Doll, J. D., Bundy, L. G., Schuler, R. T., & Holmes, B. J. (2016, January 29). *Alternative field crops manual*. Retrieved from Grain Sorghum (Milo): https://www.hort.purdue.edu/newcrop/afcm/sorghum.html

CDC. (2016, 12 10). *Colorectal cancer*. Retrieved from Center for disease control: https://www.cdc.gov/cancer/colorectal/statistics/index.htm

Chen, F., Cole, P., Mi, Z. B., & Xing, L. Y. (1993). Corn and wheat-flour consumption and mortality from esophageal cancer in Shanxi, China. *International Journal of cancer, 53*(6), 902-906.

Cheng, L., Jin, H., Qiang, Y., Wu, S., Yan, C., Han, M., . . . Xia, S. (2016). High fat diet exacerbates dextran sulfate sodium induced colitis through disturbing mucosal dendritic cell homeostasis. *International immunopharmacology, 40*, 1-10.

Choo, Y.-Y., Lee, S., Nguyen, P.-H., Lee, W., Woo, M.-H., Min, B.-S., & Lee, J.-H. (2015). Caffeoylglycolic acid methyl ester, a major constituent of sorghum, exhibits anti-inflammatory activity via the Nrf2/heme oxygenase-1 pathway. *RSC Advances, 5*, 17786-96.

Christiansen, K. (2006). *Understanding the parameters affecting lipid extraction from grain sorghum.* Lincoln: University of Nebraska-Lincoln.

Christiansen, K. L., Weller, C. L., Schlegel, V. L., Cuppett, S. L., & Carr, T. P. (2007). Extraction and Characterization of Lipids from the Kernels, Leaves, and Stalks of Nine Grain Sorghum Parent Lines. *Cereal chemistry, 84*(5), 463-70.

Christiansen, K., Weller, C., Schlegel, V., & Dweikat, I. (2008). Comparision of Lipid Extraction Methods of Food-Grade Sorghum (Sorghum biolor) Using Hexane. *Biological Engineering, 1*, 51-63.

Collins, Y., Chouchani, E. T., James, A. M., Menger, K. E., Cocheme, H. M., & Murphy, M. P. (2012). Mitochondrial redox signaling at a glance. *Journal of Cell Science, 125*, 801-6.

Cruz, R. A., Lopez, J. L., Aguilar, G. A., Garcia, H. A., Gorinstein, S., Romero, R. C., & Sanchez, M. R. (2015). Influence of Sorghum Kafirin on Serum Lipid Profile and Antioxidant Activity in Hyperlipidemic Rats (In Vitro and In Vivo Studies). *BioMed research international, 2015*, 164725.

Cuervo, A., Salazar, N., Ruas-Madiedo, P., Gueimonde, M., & González, S. (2013). Fiber from a regular diet is directly associated with fecal short-chain fatty acid concentrations in the elderly. *Nutrition research, 33*(10), 811-6.

Darvin, P., Joung, Y. H., Nipin, S. P., Kang, D. Y., Byun, H. J., Hwang, D. Y., . . . Yang, Y. M. (2015). Sorghum polyphenol suppresses the growth as well as metastasis of colon cancer xenografts through co-targeting jak2/STAT3 and PI3K/Akt/mTOR pathways. *Journal of functional food, 15*, 193-206.

de Morais Cardoso, L., Pinheiro, S., Martino, H., & Pinheiro-Sant'Ana, H. (2017). Sorghum (Sorghum bicolor L.): Nutrients, bioactive compounds, and potential impact on human health. *Critical reviews in food science and nutrition, 57*(2), 372-90.

Debray, F., Mitchell, G., Allard, P., Robinson, B., Hanley, J., & Lambert, M. (2007). Diagnostic accuracy of blood lactate-to-pyruvate molar ratio in the differential diagnosis of congenital lactic acidosis. *Clinical chemistry, 53*(5), 916-21.

Deplancke, B., & Gaskins, H. (2001). Microbial modulation of innate defense: goblet cells and the intestinal mucus layer. *The Ametican journal of clinical nutrition, 73*(6), 1131S-1141S.

Dettmer, K., & Hammock, B. (2004). Metabolomics--a new exciting field within the "omics" sciences. *Environmental health perspectives, 112*(7), A396-7.

Devi, P. S., Kumar, M. S., & Das, S. M. (2011). Evaluation of Antiproliferative Activity of Red Sorghum Bran Anthocyanin on a Human Breast Cancer Cell Line (MCF-7). *International Journal of Breast Cancer, 2011*, 891481.

Dinh, C., Yu, Y., Szabo, A., Zhang, Q., Zhang, P., & Huang, X. (2016). Bardoxolone Methyl Prevents High-Fat Diet-Induced Colon Inflammation in Mice. *The journal of histochemistry and cytochemistry, 64*(4), 237-55.

Dulin, M., Hatcher, L., Sasser, H., & Barringer, T. (2006). Policosanol is ineffective in the treatment of hypercholesterolemia: a randomized controlled trial. *The American journal of clinical nutrition, 84*(6), 1543-8.

Easlon, E., Tsang, F., Skinner, C., Wang, C., & Lin, S. (2008). The malate-aspartate NADH shuttle components are novel metabolic longevity regulators required for calorie restriction-mediated life span extension in yeast. *Genes & development, 22*(7), 931-44.

Erdelyi, I., Levenkova, N., Lin, E., Pinto, J., Lipkin, M., Quimby, F., & Holt, P. (2009). Western-style diets induce oxidative stress and dysregulate immune responses in the colon in a mouse model of sporadic colon cancer. *The journal of nutrition, 139*(11), 2072-8.

Evans, M. D., Griffiths, H. R., & Lunec, J. (1997). Reactive Oxygen Species and their Cytotoxic Mechanisms. *Advances in molecular and cell biology, 20*, 25-73.

Fillmore, N., Mori, J., & Lopaschuk, G. (2014). Mitochondrial fatty acid oxidation alterations in heart failure, ischaemic heart disease and diabetic cardiomyopathy. *British journal of pharmacology, 171*(8), 2080-90.

Fuentes, E., Báez, M., Bravo, M., Cid, C., & Labra, F. (2012). Determination of total phenolic content in olive oil samples by UV-visible spectrometry and multivariate calibration. *Food analytical methods, 5*(6), 1311-9.

Fujisawa, T., Endo, H., Tomimoto, A., Sugiyama, M., Takahashi, H., Saito, S., . . . Nakajima, A. (2008). Adiponectin suppressescolorectal carcinogenesis under the high-fat diet condition. *Gut, 57*(11), 1531-8.

Gouni-Berthold, I., & Berthold, H. K. (2002). Policosanol: clinical pharmacology and therapeutic significance of a new lipid-lowering agent. *American heart journal, 143*(2), 356-65.

Gries, T. L. (2008). *Capillary electrophoresis for metabolic profiling of inducible inflammation and anti-inflammatory properties of resveratrol in raw macrophage immortal cell lines.* Lincoln, Nebraska: University of Nebraska-Lincoln.

Gumaa, K. A., McLean, P., & Greenbaum, A. L. (1971). Compartmentation in relation to metabolic control in liver. *Essays in Biochemistry, 7*, 39-86.

Guo, W., Jiang, C., Yang, L., Li, T., Liu, X., Jin, M., . . . Wang, Y. (2016). Quantitative Metabolomic Profiling of Plasma, Urine, and Liver Extracts by 1H NMR Spectroscopy Characterizes Different Stages of Atherosclerosis in Hamsters. *Journal of proteome research, 15*(10), 3500-10.

Hartle, D. K., Greenspan, P., & Hargrove, J. L. (2011). High polyphenolic sorghum brans have much higher antioxidant and anti-inflammatory activities than wheat, rice or oat brans. *The FASEB Journal, 25*, 773.4.

Hoi, J. T., Weller, C. L., Schlegel, V. L., Cuppett, S. L., Lee, J.-Y., & Carr, T. P. (2009). Sorghum distillers dried grain lipid extract increases cholesterol excretion and decreases

plasma and liver cholesterol concentration in hamsters. *Journal of functional foods, 1*(4), 381-6.

Hotamisligil, G., & Erbay, E. (2008). Nutrient sensing and inflammation in metabolic diseases. *Nature review immulology, 8*(12), 923-34.

Hwang, J.-M., Choi, K.-C., Bang, S.-J., Son, Y.-O., Kim, B.-T., Kim, D.-H., . . . Lee, J.-C. (2013). Anti-oxidant and Anti-inflammatory Properties of Methanol Extracts from Various Crops. *Food science and biotechnoloby, 22*(S), 265-72.

Hwang, K. T., Cuppett, S. L., Weller, C. L., & Hanna, M. A. (2002). HPLC of grain sorghum wax classes highlighting separation of aldehydes from wax esters and steryl esters. *Journal of separation science, 25*(9), 619-23.

Hwang, K. T., Kim, J. E., & Weller, C. L. (2005). Policosanol Contents and Compositions in Wax-Like Materials Extracted from Selected Cereals of Korean Origin. *Cereal chemistry, 82*(3), 242-5.

Hwang, K. T., Weller, C. L., Cuppett, S. L., & Hanna, M. A. (2004). Policosanol Contents and Composition of Grain Sorghum Kernels and Dried Distillers Grains. *Cereal chemistry, 81*(3), 345-9.

Hwang, S., Kim, H., Jung, H., Kim, J., Choi, D., Hur, J., . . . Huh, T. (2008). Beneficial effects of beta-sitosterol on glucose and lipid metabolism in L6 myotube cells are mediated by AMP-activated protein kinase. *Biochemical and biophysical research communications, 377*(4), 1253-8.

Jakobsdottir, G., Xu, J., Molin, G., Ahrné, S., & Nyman, M. (2013). High-Fat Diet Reduces the Formation of Butyrate, but Increases Succinate, Inflammation, Liver Fat and Cholesterol in Rats, while Dietary Fibre Counteracts These Effects. *PloS one, 8*(11), e80476.

James, A., Yvonne, C., Logan, A., & Murphy, M. (2012). Mitochondrial oxidative stress and the metabolic syndrome. *Trends in Endocrinology and Metabolism, 9*, 429-34.

Jia, G., Aroor, A. R., Martinez-Lemus, L. A., & Sowers, J. R. (2014). Overnutrition, mTOR signaling, and cardiovascular diseases. *American journal of physiology. Regulatory, integrative and comparative physiology, 307*(10), R1198-206.

Jiang , C., Yang , K., Yang , L., Miao, Z., Wang, Y., & Zhu, H. (2013). A (1)H NMR-Based Metabonomic Investigation of Time-Related Metabolic Trajectories of the Plasma, Urine and Liver Extracts of Hyperlipidemic Hamsters. *PloS one, 8*(6), e66786.

Jones, W., & Bianchi, K. (2015). Aerobic glycolysis: beyond proliferation. *Frontiers in Immunology, 6*, 227.

Junio, H., Sy-Cordero, A., Ettefagh, K., Burns, J., Micko, K., Graf, T., . . . Cech, N. (2011). Synergy-Directed Fractionation of Botanical Medicines: A Case Study with Goldenseal (Hydrastis canadensis). *Journal of natural products, 74*(7), 1621-9.

Kane, D. (2014). Lactate oxidation at the mitochondria: a lactate-malate-aspartate shuttle at work. *Frontiers in neuroscience, 8*(366). doi:doi: 10.3389/fnins.2014.00366

Kang, P., Liu, Y., Zhu, H., Li, S., Shi, H., Chen, F., . . . Yi, D. (2015). The effect of aspartate on the energy metabolism in the liver of weanling pigs challenged with lipopolysaccharide. *European journal of nutrition, 54*(4), 581-8.

Kell, D. (2006). Systems biology, metabolic modelling and metabolomics in drug discovery and development. *Drug discovery today, 11*(23-24), 1085-92.

Khan, I., Yousif, A. M., Johnson, S. K., & Gamlath, S. (2015). Acute effect of sorghum flour-containing pasta on plasma total polyphenols, antioxidant capacity and oxidative stress markers in healthy subjects: A randomised controlled trial. *Clinical Nutrition, 34*(3), 415-21.

Kim, E., Kim, S., & Park, Y. (2015). Sorghum extract exerts cholesterol-lowering effects through the regulation of hepatic cholesterol metabolism in hypercholesterolemic mice. *International journal of food science and nutrition, 66*(3), 308-13.

Kim, I., Myung, S., Do, M., Ryu, Y., Kim, M., Do, E., . . . Kim, J. (2010). Western-style diets induce macrophage infiltration and contribute to colitis-associated carcinogenesis. *Journal of gastroenterology and hepatology, 25*(11), 1785-94.

Kim, J., & Park, Y. (2012). Anti-diabetic effect of sorghum extract on hepatic gluconeogenesis of streptozotocin-induced diabetic rats. *Nutrition & metabolism, 9*(1), 106.

Kim, K., Gu, W., Lee, I., Joh, E., & Kim, D. (2012). High fat diet-induced gut microbiota exacerbates inflammation and obesity in mice via the TLR4 signaling pathway. *PloS one, 7*(10), e47713.

Koivunen, P., Hirsilä, M., Remes, A., Hassinen, I., Kivirikko, K., & Myllyharju, J. (2007). Inhibition of hypoxia-inducible factor (HIF) hydroxylases by citric acid cycle intermediates: possible links between cell metabolism and stabilization of HIF. *The Journal of biological chemistry, 282*(7), 4524-32.

Korshunov, S. S., Skulachev, V. P., & Starkov, A. A. (1997). High protonic potential actuates a mechanism of production of reactive oxygen species in mitochondria. *FEBS letters, 416*(1), 15-8.

Korshunov, S. S., Skulachev, V. P., & Starkov, A. A. (1997). High protonic potential actuates a mechanism of production of reactive oxygen species in mitochondria. *FEBS letters, 416*(1), 15-8.

Kowalski, G., De Souza, D., Burch, M., Hamley, S., Kloehn, J., Selathurai, A., . . . Bruce, C. (2015). Application of dynamic metabolomics to examine in vivo skeletal muscle glucose metabolism in the chronically high-fat fed mouse. *Biochemical and biophysical research communications, 462*(1), 27-32.

Kwong, L. K., & Sohal, R. S. (1998). Substrate and site specificity of hydrogen peroxide generation in mouse mitochondria. *Archives of Biochemistry and Biophysics, 350*(1), 118-26.

Lactate to Pyruvate Ratio, Whole Blood. (2017, April 24). Retrieved from Laboratory Test Directory: http://ltd.aruplab.com/Tests/Pub/2007935

Larrain, R. E., Richards, M. P., Schaefer, D. M., & Reed, J. D. (2007). Growth performance and muscle oxidation in rats fed increasing amounts of high-tannin sorghum. *Journal of animal science, 85*(12), 3276-84.

Lecomte, V., Kaakoush, N., Maloney, C., Raipuria, M., Huinao, K., Mitchell, H., & Morris, M. (2015). Changes in gut microbiota in rats fed a high fat diet correlate with obesity-associated metabolic parameters. *PLoS One, 10*(5), e0126931.

Lee, B. (2013). *Effects of grain sorghum wax and oil on cholesterol levels, gut microbiota, and tissue metabolic fingerprints / profiles of a hamster model with diet-induced hypercholesterolemia.* Lincoln, Nebraska: University of Nebraska-Lincoln.

Lee, B. H., Carr, T. P., Weller, C. L., Cuppett, S., Dweikat, I. M., & Schlegel, V. (2014). Grain sorghum whole kernel oil lowers plasma and liver cholesterol in male hamsters with minimal wax involvement. *Journal of functional foods, 7*, 709-18.

Lee, B., Weller, C., Cuppett, S., Carr, T., Walter, J., Martínez, I., & Schlegel, V. (2011). Grain sorghum lipids: extraction, characterization, and health potential. In *Advances in cereal science: implications to food processing and health promotion* (pp. 149-70).

Lee, J., Lee, S., Kim, B., Seo, W., Jia, Y., Wu, C., . . . Lee, S. (2015). Barley sprout extract containing policosanols and polyphenols regulate AMPK, SREBP2 and ACAT2 activity and cholesterol and glucose metabolism in vitro and in vivo. *Food research international, 72*, 174-83.

Leguizamón, C., Weller, C. L., Schlegel, V. L., & Carr, T. P. (2009). Plant Sterol and Policosanol Characterization of Hexane Extracts from Grain Sorghum, Corn and their DDGS. *Journal of the American oil chemists' society, 86*(7), 707-16.

Lewis, J. B., Taddeo, S. S., McDonough, C. M., Rooney, L. W., Carroll, R. J., & Tunner, N. D. (2008). Sorghum bran varieties differentially influence endogenous antioxidant enzymes to protect against oxidative stress during colon carcinogenesis. *The FASEB Journal, 22*, 887.7.

Lewis, J. B., Taddeo, S. S., McDonough, C. M., Rooney, L. W., Carroll, R. J., & Turner, N. D. (2008). Sorghum bran varieties differentially influence endogenous antioxidant enzymes to protect against oxidative stress during colon carcinogenesis. *The FASEB Journal, 22*, 888.7.

Li, Z., Ding, L., Li, J., Xu, B., Yang, L., Bi, K., & Wang, Z. (2015). ^{1}H-NMR and MS based metabolomics study of the intervention effect of curcumin on hyperlipidemia mice induced by high-fat diet. *PloS one, 10*(3), e0120950.

Lichtenthaler, H., & Buschmann, C. (2001). Chlorophylls and carotenoids: measurement and characterization by UV-VIS spectroscopy. In *Current protocols in food analytical chemistry* (pp. F4.3.1-F4.3.8). John Wiley & Sons, Inc.

Lin, Y., Rudrum, M., van der Wielen, R., Trautwein, E., Mcneill, G., Sierksma, A., & Meijer, G. (2004). Wheat germ policosanol failed to lower plasma cholesterol in subjects with normal to mildly elevated cholesterol concentrations. *Metabolism: clinical and experimental, 53*(10), 1309-14.

Lionetti, L., Mollica, M. P., Lombardi, A., Cavaliere, G., Gifuni, G., & Barletta, A. (2009). From chronic overnutrition to insulin resistance: The role of fat-storing capacity and inflammation. *Nutrition, metabolism and cardiovascular diseases, 19*(2), 146-52.

Lodish, H., Berk, A., Zipursky, S. L., Matsudaira, P., Baltimore, D., & Darnell, J. (2000). Section 16.2, Electron transport and oxidative phosphorylation. In *Molecular cell biology (4th edition).* W. H. Freeman, New York.

Lushckak, V. (2012). Glutathione homeostasis and functions: potential targets for medical interventions. *Journal of amino acids, 2012*, 736837.

Ma, X., Torbenson, M., Hamad, A., Soloski, M., & Li, Z. (2008). High-fat diet modulates non-CD1d-restricted natural killer T cells and regulatory T cells in mouse colon and exacerbates experimental colitis. *Clinical and experimental immunology, 151*(1), 130-8.

Martínez, I., Perdicaro, D. J., Brown, A. W., Hammons, S., Carden, T. J., Carr, T. P., . . . Walter, J. (2013). Diet-induced alterations of host cholesterol metabolism are likely to affect the gut microbiota composition in hamsters. *Applied and environmental microbiology, 79*(2), 516-24.

Martínez, I., Wallace, G., Zhang, C., Legge, R., Benson, A. K., Carr, T. P., . . . Walter, J. (2009). Diet-Induced Metabolic Improvements in a Hamster Model of Hypercholesterolemia Are Strongly Linked to Alterations of the Gut Microbiota. *Applied and environmental microbiology, 75*(12), 4175-84.

Massey, A. R., Reddivari, L., & Vanamala, J. (2014). The Dermal Layer of Sweet Sorghum (Sorghum bicolor) Stalk, a Byproduct of Biofuel Production and Source of Unique 3-Deoxyanthocyanidins, Has More Antiproliferative and Proapoptotic Activity than the Pith in p53 Variants of HCT116 and Colon Cancer Stem Cel. *Journal of agricultural and food chemistry, 62*, 3150−9.

McGarry, J. D., & Dobbins, R. L. (1999). Fatty acids, lipotoxicity and insulin. *Diabetologia, 42*(2), 128-38.

Metcalfe, L., Schmitz, A., & Pelka, J. (1966). Rapid Preparation of Fatty Acid Esters from Lipids for Gas Chromatographic Analysis. *Analytical chemistry, 38*(3), 514-5.

Misawa, E., Tanaka, M., Nomaguchi, K., Nabeshima, K., Yamada, M., Toida, T., & Iwatsuki, K. (2012). Oral ingestion of aloe vera phytosterols alters hepatic gene expression profiles and ameliorates obesity-associated metabolic disorders in zucker diabetic fatty rats. *Journal of agricultural and food chemistry, 60*(11), 2799-806.

Misawa, E., Tanaka, M., Nomaguchi, K., Yamada, M., Toida, T., Takase, M., . . . Kawada, T. (2008). Administration of phytosterols isolated from Aloe vera gel reduce visceral fat mass and improve hyperglycemia in Zucker diabetic fatty (ZDF) rats. *Obesity research & clinical practice, 2*(4), 239-45.

Mittal, M., Siddiqui, M. R., Tran, K., Reddy, S. P., & Malik, A. B. (2014). Reactive oxygen species in inflammation and tissue injury. *Antioxidants & redox signaling, 20*(7), 1126-67.

Morgan, M. J., & Liu, Z.-g. (2011). Crosstalk of reactie oxygen species and NF-kB siganling. *Cell Research, 21*(1), 103-15.

Murakami, Y., Tanabe, S., & Suzuki, T. (2016). High-fat Diet-induced Intestinal Hyperpermeability is Associated with Increased Bile Acids in the Large Intestine of Mice. *Journal of food science, 81*(1), H216-22.

Murphy, K., Saint, D., & Howe, P. (2008). Lack of effect of sugar cane and sunflower seed policosanols on plasma cholesterol in rabbits. *Journal of the American college of nutrition, 27*(4), 476-84.

Murphy, M. (2009). How mitochondria produce reactive oxygen species. *The Biochemical Journal, 417*, 1-13.

Nava, G., Carbonero, F., Croix, J., Greenberg, E., & Gaskins, H. (2012). Abundance and diversity of mucosa-associated hydrogenotrophic microbes in the healthy human colon. *The ISME journal, 6*(1), 57-70.

Neucere, N. J., & Sumrell, G. (1980). Chemical Composition of Different Varieties of Grain Sorghum. *Journal of agricultural and food chemistry, 28*(1), 19-21.

Nguyen, P.-H., Zhao, B. T., Lee, J. H., Kim, Y. H., Min, B. S., & Woo, M. H. (2015). Isolation of benzoic and cinnamic acid derivatives from the grains of Sorghum bicolor and their inhibition of lipopolysaccharide-induced nitric oxide production in RAW 264.7 cells. *Food chemistry, 168*, 512-9.

Nikolaev, E., Burgard, A., & Maranas, C. (2005). Elucidation and structural analysis of conserved pools for genome-scale metabolic reconstructions. *Biophysical journal, 88*(1), 37-49.

Nishikawa, T., Edelstein, D., Du, X., Yamagishi, S.-i., Matsumura, T., Kaneda, Y., . . . Brownlee, M. (2000). Normalizing mitochondrial superoxide production blocks three pathways of hyperglycaemic damage. *Nature, 404*(6779), 787-90.

Oboh, G., Akomolafe, T. L., & Adetuyi, A. O. (2010). Inhibition of Cyclophosphamide-Induced Oxidative Stress in Brain by Dietary Inclusion of Red Dye Extracts from Sorghum (Sorghum bicolor) Stem. *Journal of medicinal food, 13*(5), 1075-80.

Padidar, S., Farquharson, A., Williams, L., Kearney, R., Arthur, J., & Drew, J. (2012). High-fat diet alters gene expression in the liver and colon: links to increased development of aberrant crypt foci. *Digestive diseases and sciences, 57*(7), 1866-74.

Park, J. H., Darvin, P., Lim, E. J., Joung, Y. H., Hong, D. Y., Park, E. U., . . . Yang, Y. M. (2012). Hwanggeumchal sorghum Induces Cell Cycle Arrest, and Suppresses Tumor Growth and Metastasis through Jak2/STAT Pathways in Breast Cancer Xenografts. *PloS One, 7*(7), e40531.

Paturi, G., Butts, C., Monro, J., Nones, K., Martell, S., Butler, R., & Sutherland, J. (2010). Cecal and colonic responses in rats fed 5 or 30% corn oil diets containing either 7.5% broccoli dietary fiber or microcrystalline cellulose. *Journal of agricultural and food chemistry, 58*(10), 6510-5.

Piironen, V., Toivo, J., & Lampi, A. (2002). Plant sterols in cereals and cereal products. *Cereal chemistry, 79*(1), 148-54.

Ravasz, E., Somera, A., Mongru, D., Oltvai, Z., & Barabási, A. (2002). Hierarchical organization of modularity in metabolic networks. *Science, 297*(5586), 1551-5.

Richardson, A., Yang, C., Osterman, A., & Smith, J. (2008). Central carbon metabolism in the progression of mammary carcinoma. *Breast cancer research and treatment, 110*(2), 297-307.

Ríos-Covián, D., Ruas-Madiedo, P., Margolles, A., Gueimonde, M., de Los Reyes-Gavilán, C., & Salazar, N. (2016). Intestinal Short Chain Fatty Acids and their Link with Diet and Human Health. *Frontiers in microbiology, 7*, 185.

Ritchie, L. E., Carroll, R. J., Weeks, B. R., McDonough, C. M., Dykes, L., Rooney, L. W., & Turner, N. D. (2011). Reduction in DSS-induced enhancement of colonic injury and NF-{kappa}B activation in rats consuming a diet containing black sorghum bran. *The FASEB Journal, 25*, 977.4.

Ritchie, L. E., Carroll, R., Weeks, B., Rooney, L., & Turner, N. D. (2012). Novel sorghum brans containing bioactive compounds alter the production of microbial secondary metabolites in response to a DSS-induced chronic inflammatory state. *The FASEB Journal, 26*, 823.36.

Ritchie, L. E., Sturino, J. M., Azcarate-Peril, M. A., & Turner, N. D. (2013). Novel sorghum brans containing bioactive compounds alter colon microbiota in response to a DSS-induced chronic inflammatory state. *The FASEB Jouranl, 27*, 247.2.

Ritchie, L. E., Sturino, J. M., Carroll, R. J., Rooney, L. W., Azcarate-Peril, M. A., & Turner, N. D. (2015). Polyphenol-rich sorghum brans alter colon microbiota and impact species diversity and species richness after multiple bouts of dextran sodium sulfate-induced colitis. *FEMS Microbiology ecology, 91*(3), pii: fiv008.

Robinson, B. (2001). 100: Lactic Acidemia: Disorders of Pyruvate Carboxylase and Pyruvate Dehydrogenase. In *The Metabolic and Molecular Bases of Inherited Disease, 8th ed* (pp. 2275-95). New York: McGraw-Hill New York.

Rooney, L., Dahlberg, J., Bean, S., Weller, C., Turner, N., Awika, J., . . . Smail, V. (2010). *Sorghum: An Ancient, Healthy and Nutritious Old World Cereal*. (E. C. Henley, Editor, & United sorghum checkoff program) Retrieved 04 27, 2016, from sorghumcheckoff.com: http://sorghumcheckoff.com/wp-content/uploads/2012/06/SorghumAncientGrainFinal12-8-11.pdf

Rosca, M. G., Vazquez, E. J., Chen, Q., Kerner, J., Kern, T. S., & Hoppel, C. L. (2012). Oxidation of Fatty Acids Is the Source of Increased Mitochondrial Reactive Oxygen Species Production in Kidney Cortical Tubules in Early Diabetes. *Diabetes, 61*(8), 2074-2083.

Satapati, S., Sunny, N., Kucejova, B., Fu, X., He, T., Méndez-Lucas, A., . . . Burgess, S. (2012). Elevated TCA cycle function in the pathology of diet-induced hepatic insulin resistance and fatty liver. *Journal of lipid research, 53*(6), 1080-92.

Selak, M., Armour, S., MacKenzie, E., Boulahbel, H., Watson, D., Mansfield, K., . . . Gottlieb, E. (2005). Succinate links TCA cycle dysfunction to oncogenesis by inhibiting HIF-alpha prolyl hydroxylase. *Cancer cell, 7*(1), 77-85.

Serna-Saldivar, S., & Rooney, L. W. (1994). Structure and chemistry of sorghum and millets. In *Sorghum and Millets: Chemistry and Technology* (pp. 67-127).

Shen, W., Wolf, P., Carbonero, F., Zhong, W., Reid, T., Gaskins, H., & Mclntosh, M. (2014). Intestinal and systemic inflammatory responses are positively associated with sulfidogenic bacteria abundance in high-fat-fed male C57BL/6J mice. *The Journal of nutrition, 144*(8), 1181-7.

Shi, L., & Tu, B. (2015). Acetyl-CoA and the regulation of metabolism: mechanisms and consequences. *Current opinion in cell biology, 33*, 125-31.

Shim, T.-J., Kim, T. M., Jang, K. C., Ko, J.-Y., & Kim, D. J. (2013). Toxicological evaluation and anti-inflammatory activity of a golden gelatinous sorghum bran extract. *Bioscience, biotechonology, and biochemistry, 77*(4), 697-705.

Singh, D., Li, L., & Porter, T. (2006). Policosanol inhibits cholesterol synthesis in hepatoma cells by activation of AMP-kinase. *The journal of phamacology and experimental therapeutics, 318*(3), 1020-6.

Singh, V., Moreau, R. A., & Hicks, K. B. (2003). Yield and Phytosterol Composition of Oil Extracted from Grain Sorghum and Its Wet-Milled Fractions. *Cereal chemistry, 80*(2), 126-9.

Sparks, L. M., Xie, H., Koza, R. A., Mynatt, R., Hulver, M. W., Bray, G. A., & Smith, S. R. (2005). A High-Fat Diet Coordinately Downregulates Genes Required for Mitochondrial Oxidative Phosphorylation in Skeletal Muscle. *Diabetes, 54*(7), 1926-33.

Stefoska-Needham, A., Beck, E. J., Johnson, S. K., & Tapsell, L. C. (2015). Sorghum: An Underutilized Cereal Whole Grain with the Potential to Assist in the Prevention of Chronic Disease. *Food reviews international, 31*(4), 401-37.

Strober, W., Fuss, I., & Blumberg, R. (2002). The immunology of mucosal models of inflammation. *Annual review of immunology, 20*, 495-549.

Suganyadevi, P., Saravanakumar , K. M., & Mohandas , S. (2013). The antiproliferative activity of 3-deoxyanthocyanins extracted from red sorghum (Sorghum bicolor) bran through P53-dependent and Bcl-2 gene expression in breast cancer cell line. *Life sciences, 92*(6-7), 379-82.

Sunny, N., Parks, E., Browning, J., & Burgess, S. (2011). Excessive hepatic mitochondrial TCA cycle and gluconeogenesis in humans with nonalcoholic fatty liver disease. *Cell metabolism, 14*(6), 804-10.

Takahashi, H., Takayama, T., Yoneda, K., Endo, H., Iida, H., Suqiyama, M., . . . Nakajima, A. (2009). Association of visceralfat accumulation and plasma adiponectin with rectal dysplasticaberrant crypt foci in a clinical population. *Cancer science, 100*(1), 29-32.

Taubes, G. (2012). Unraveling the Obesity-Cancer Connection. *Science, 335*(6064), 28-32.

Teixeira, L., Leonel, A., Aquilar , E., Batista, N., Alves, A., Coimbra, C., . . . Alvarez Leite, J. (2011). The combination of high-fat diet-induced obesity and chronic ulcerative colitis reciprocally exacerbates adipose tissue and colon inflammation. *Lipids in health and disease, 10*, 204.

Test ID: PYR. (2017, April 24). Retrieved from Mayo Medical Laboratories: http://www.mayomedicallaboratories.com/test-catalog/Clinical+and+Interpretive/8657

Tunner, N. D., Diaz, A., Taddeo, S. S., Vanamala, J., McDonough, C. M., Dykes, L., . . . Rooney, L. W. (2006). Bran from black or brown sorghum suppresses colon carcinogenesis. *The FASEB Journal, 20*, A599.

USDA. (2016). *Crop Production 2015 Summary*`. National Agricultural Statistics Service.

van der Werf, M., & Venema, K. (2001). Bifidobacteria: Genetic Modification and the Study of Their Role in the Colon. *Journal of agricultural and food chemistry, 49*(1), 378–83.

van Rensburg, S. J. (1981). Epidemiological and dietary evidence for a specific nutritional predisposition to esophageal cancer. *Journal of the national cancer institute, 67*(2), 243-251.

Vettor, R., Lombardi, A. M., Fabris, R., Pagano, C., Cusin, I., Rohner-Jeanrenaud , F., . . . Jeanrenaud, B. (1997). Lactate infusion in anesthetized rats produces insulin resistance in heart and skeletal muscles. *Metabolism: clinical and experimental, 46*(6), 684-90.

Wallace, D. C. (1992). Diseases of the Mitochondrial DNA. *Annual Review of Biochemistry, 61*, 1175-212.

Wang, L., Weller, C. L., & Hwang, K. T. (2005). Extraction of lipids from grain sorghum DDG. *Transactions of the ASAE, American Society of Agricultural Engineers, 48*(5), 1883-8.

Wang, L., Weller, C. L., Schlegel, V. L., Carr, T. P., & Cuppett, S. L. (2007). Comparison of supercritical CO2and hexaneextraction of lipids from sorghum distillers grains. *European journal of lipid science and technology, 109*(6), 567-74.

Wang, X., Liu, Y., Li, S., Pi, D., Zhu, H., Hou, Y., . . . Leng, W. (2015). Asparagine attenuates intestinal injury, improves energy status and inhibits AMP-activated protein kinase signalling pathways in weaned piglets challenged with Escherichia coli lipopolysaccharide. *The British journal of nutrition, 114*(4), 553-65.

Warburg, O., & Negelein, E. (1927). The metabolism of tumors in the body. *The Journal of General Physiology, 8*(6), 519-30.

Weljie, A., Dowlatabadi, R., Miller, B., Vogel, H., & Jirik, F. (2007). An Inflammatory Arthritis-Associated Metabolite Biomarker Pattern Revealed by 1H NMR Spectroscopy. *Journal of proteome research, 6*(9), 3456-64.

Wellen, K. E., & Thompson, C. B. (2010). Cellular metabolic stress: considering how cells respond to nutrient excess. *Molecular cell, 40*(2), 323-32.

West, A. P., Shadel, G. S., & Ghosh, S. (2011). Mitochondria in innate immune responses. *Nature Reviews Immunology, 11*, 389-402.

White, T., Bursten, S., Federighi, D., Lewis, R., & Nudelman, E. (1998). High-resolution separation and quantification of neutral lipid and phospholipid species in mammalian cells and sera by multi-one-dimensional thin-layer chromatography. *Analytical biochemistry, 258*(1), 109-17.

Williamson, J. R., Chang, K., Frangos, M., Hasan, K. S., Ido, Y., Kawamura, T., . . . Tilton, R. G. (1993). Hyperglycemic Pseudohypoxia and Diabetic Complications. *Diabetes, 42*(6), 801-813.

Winkler, J., Rennick, K., Eller, F., & Vaughn, S. (2007). Phytosterol and tocopherol components in extracts of corn distiller's dried grain. *Journal of agricultural and food chemistry, 55*(16), 6482-6.

Wong, M., Timms, R., & Goh, E. (1988). Colorimetric determination of total tocopherols in palm oil, olein and stearin. *Journal of the American oil chemists society, 65*, 258.

Wu, D., & Cederbaum, A. I. (2003). Alcohol, oxidative stress, and free radical damage. *Alcohol research & health, 27*(4), 277-84.

Wu, L., Huang, Z., Qin, P., Yao, Y., Meng, X., Zou, J., . . . Ren, G. (2011). Chemical Characterization of a Procyanidin-Rich Extract from Sorghum Bran and Its Effect on Oxidative Stress and Tumor Inhibition in Vivo. *Journal of agricultural and food chemistry, 59*(16), 8609–15.

Yan, L.-J. (2014). Pathogenesis of Chronic Hyperglycemia: From Reductive Stress to Oxidative Stress. *Journal of diabetes research, 2014*, 137919.

Yang, L., Allred, K. F., Dykes, L., Allred, C. D., & Awika, J. M. (2015). Enhanced action of apigenin and naringenin combination on estrogen receptor activation in non-malignant colonocytes: implications on sorghum-derived phytoestrogens. *Food & function, 6*(3), 749-55.

Yang, L., Allred, K. F., Geera, B., Allred, C. D., & Awika, J. M. (2012). Sorghum phenolics demonstrate estrogenic action and induce apoptosis in nonmalignant colonocytes. *Nutrition and cancer, 64*(3), 419-27.

Yang, L., Browning, J. D., & Awika, J. M. (2009). Sorghum 3-deoxyanthocyanins possess strong phase II enzyme inducer activity and cancer cell growth inhibition properties. *Journal of agricultural and food chemistry, 57*(5), 1797-804.

Zha, W., A, J., Wang, G., Yan, B., Gu, S., Zhu, X., . . . Ren, H. (2009). Metabonomic characterization of early atherosclerosis in hamsters with induced cholesterol. *Biomarkers, 14*(6), 372-80.

Zhang, X., Zhang, G., Zhang, H., Karin, M., Bai, H., & Cai, D. (2008). Hypothalamic IKKβ/NF-κB and ER Stress Link Overnutrition to Energy Imbalance and Obesity. *Cell, 135*(1), 61-73.

Zhou, C., Li, G., Li, Y., Gong, L., Huang, Y., Shi, Z., . . . Sun, C. (2015). A high-throughput metabolomic approach to explore the regulatory effect of mangiferin on metabolic network disturbances of hyperlipidemia rats. *Molecular biosystems, 11*(2), 418-33.

Zitka, O., Skalickova, S., Gumulec, J., Masarik, M., Adem, V., Hubalek, J., . . . Kizek, R. (2012). Redox status expressed as GSH:GSSG ratio as a marker for oxidative stress in paediatric tumour patients. *Oncology letters*, *4*(6), 1247-53.

Appendix

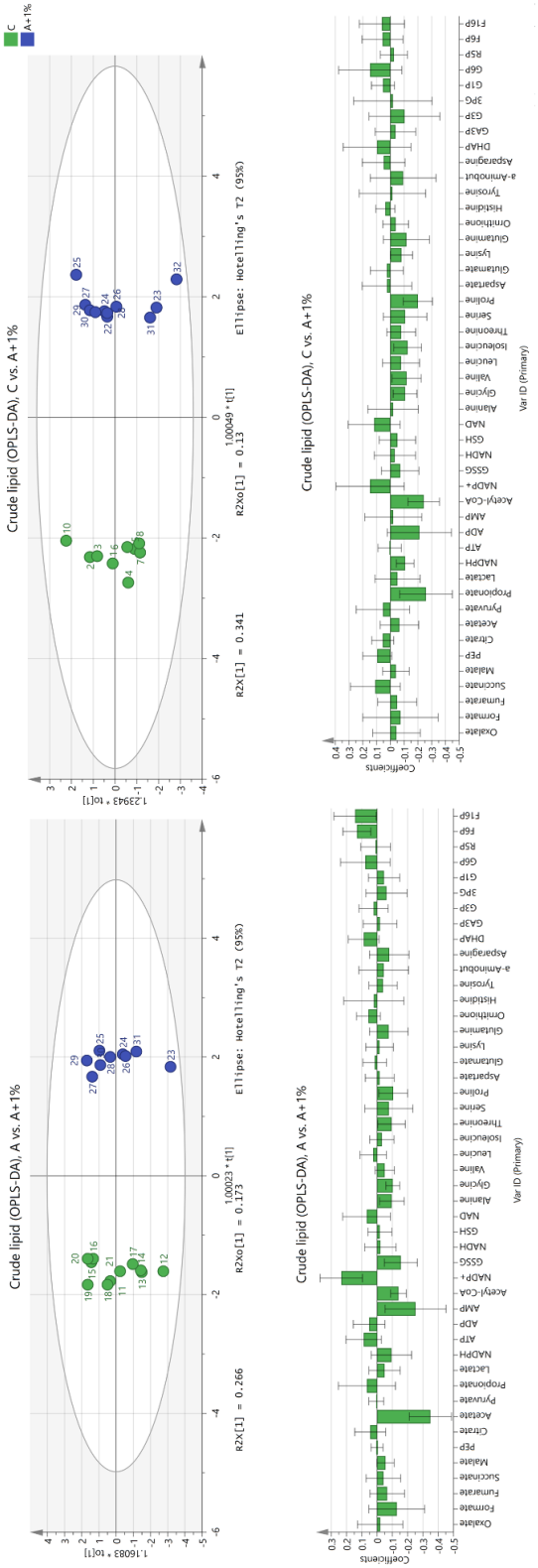

Figure 20A Effect of 1% GS-CL on metabolomics. (A)Score plot (upper, R2X=0.592, R2Y=0.993, Q2=0.946) and coefficient plot (lower) for HF and 1% groups. Positive bars (± SEM) of coefficient plot donate metabolites significantly increased when diet switch from HF to HF+1%. (B)Score plot (upper, R2X=0.67,R2Y=0.989,Q2=0.908) and coefficient plot (lower) for control and 1% groups. Positive bars (± SEM) of coefficient plot donate metabolites significantly increased when diet switch from control to HF+1%.

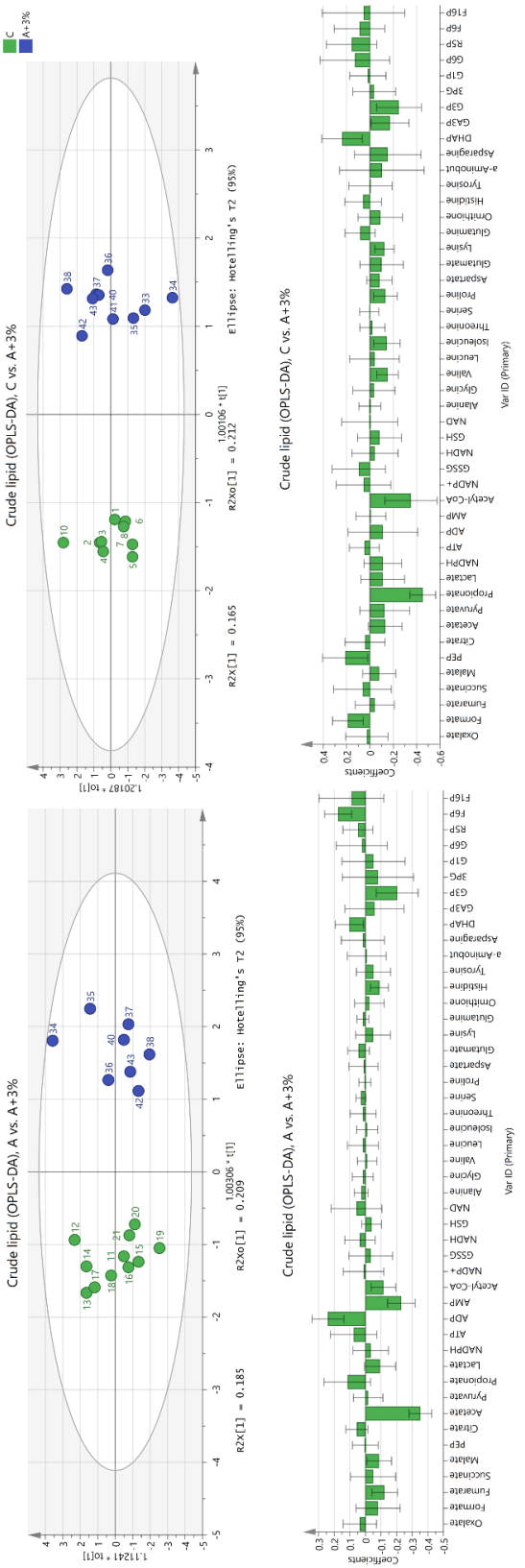

Figure 21A Effect of 3% GS-CL on metabolomics. (A)Score plot (upper, R2X=0.393, R2Y=0.951, Q2=0.859) and coefficient plot (lower) for HF and 3% groups. Positive bars (± SEM) of coefficient plot donate metabolites significantly increased when diet switch from HF to HF+3%. (B)Score plot (upper, R2X=0.591,R2Y=0.983,Q2=0.848) and coefficient plot (lower) for control and 1% groups. Positive bars (± SEM) of coefficient plot donate metabolites significantly increased when diet switch from control to HF+3%.

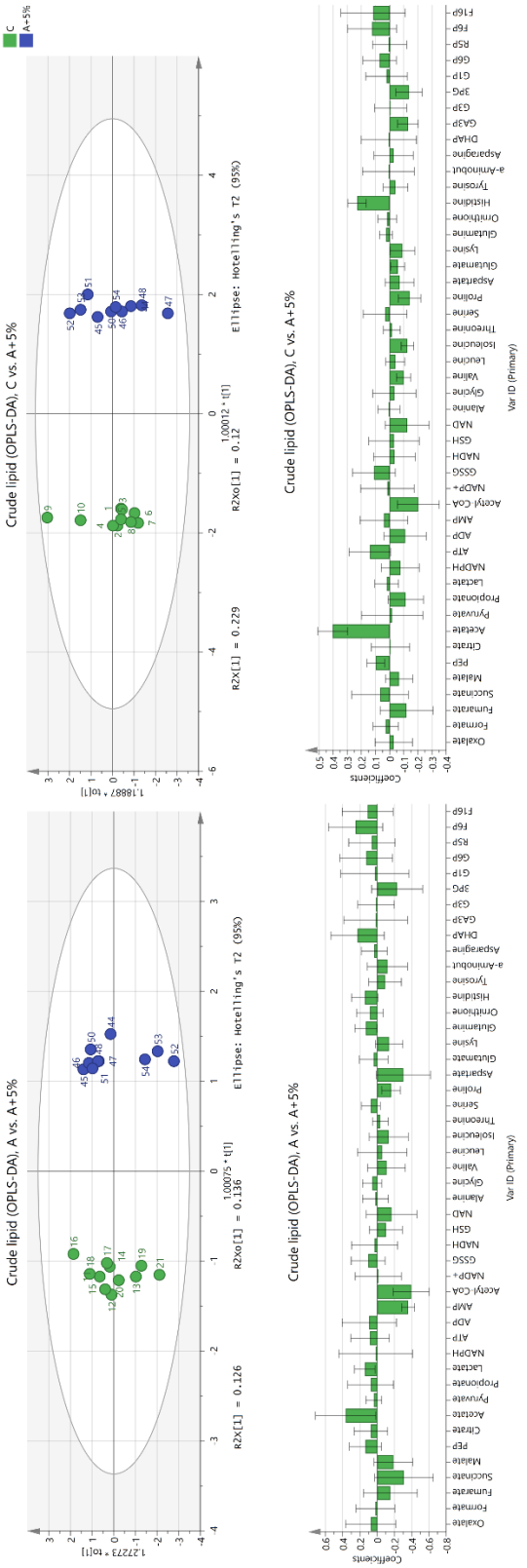

Figure 22A Effect of 5% GS-CL on metabolomics. (A)Score plot (upper, R2X=0.616, R2Y=0.99, Q2=0.784) and coefficient plot (lower) for HF and 5% groups. Positive bars (± SEM) of coefficient plot donate metabolites significantly increased when diet switch from HF to HF+5%. (B)Score plot (upper, R2X=0.742,R2Y=0.997,Q2=0.951) and coefficient plot (lower) for control and 1% groups. Positive bars (± SEM) of coefficient plot donate metabolites